



**UNIVERSITA' DEGLI STUDI DI MILANO**

**SCUOLA DI DOTTORATO IN SCIENZE AMBIENTALI**

**DIPARTIMENTO DI BIOSCIENZE**

**DOTTORATO IN SCIENZE AMBIENTALI**

**XXXII CICLO**

**PHOSPHORUS RECOVERY FROM THE LIQUID  
FRACTION OF DIGESTATES BY CRYSTALLIZATION OF  
STRUVITE**

**PhD STUDENT: Sara Zangarini**

**TUTOR: Fulvia Tambone**

## TABLE OF CONTENT

### 1. INTRODUCTION

1.1 Background.....	4
1.2 Research context and objectives.....	7

### 2. LITERATURE REVIEW: LOW-COST STRATEGIES FOR PHOSPHORUS REMOVAL FROM ANIMAL MANURE

2.1 Introduction.....	9
2.2 Chemical precipitation.....	12
2.2.1 Magnesium-based precipitation.....	12
2.2.2 Calcium-based precipitation.....	17
2.3 Electrocoagulation.....	18
2.4 Pyrolysis and Biochar.....	20
2.5 Struvite crystallization for P recovery from by-products.....	22

### 3. MATERIALS AND METHODS

3.1 Precipitation tests.....	28
3.2 Crystallization system experimental set-up.....	29
3.2.1 Reactor working principles and procedures.....	29
3.2.2 Influent solutions.....	31
3.3 DM, TKN and total P breakdown calculations.....	32
3.4 Sample characterization.....	32
3.4.1 Total Kjeldhal Nitrogen (TKN) analyses.....	33
3.4.2 Total phosphorus analyses.....	33
3.4.3 Total Organic Carbon (TOC).....	33
3.4.4 Total solids(TS) determination.....	33
3.4.5 Optical and X-ray diffraction analyses.....	34
3.5 Agronomic experimentation groundwork.....	34
3.5.1 Fertilizing product characterization: P speciation.....	34
3.5.2 Pot trials set-up.....	35

### 4. RESULTS AND DISCUSSION

4.1 Batch results.....	37
4.2 Influent solution characterization.....	39
4.3 Swine manure test performances.....	40
4.3.1 Crystallizer precipitation test.....	40
4.3.2 repartition of dry matter phosphorus and nitrogen-phosphorus.....	46
4.3.3 Optical microscopy analyses on the recovered product.....	48
4.3.4 X-ray diffraction (XRD) analyses.....	49
4.3.5 Agronomic performances.....	49
4.3.6 Phosphorus speciation.....	50

<b>4.4 Cattle manure test performances</b> .....	51
4.4.1 <i>Crystallizer precipitation test</i> .....	51
4.4.2 <i>repartition of dry matter phosphorus and nitrogen-phosphorus</i> .....	53
4.4.3 <i>Optical microscopy analyses on the recovered product</i> .....	54
4.4.4 <i>X-ray diffraction (XRD) analyses</i> .....	54
4.4.5 <i>Agronomic performances</i> .....	55
<b>4.5 OFMSW manure test performances</b> .....	57
4.5.1 <i>Crystallizer precipitation test</i> .....	57
4.5.2 <i>repartition of dry matter phosphorus and nitrogen-phosphorus</i> .....	58
4.5.3 <i>Optical microscopy analyses on the recovered product</i> .....	59
4.5.4 <i>X-ray diffraction (XRD) analyses</i> .....	60
4.5.5 <i>Agronomic performances</i> .....	61
 <b>5. CONCLUSIONS</b> .....	 63
 <b>REFERENCES</b> .....	 64

# 1. INTRODUCTION

## 1.1 Background

Today, the world population is progressively increasing, adding about 83 million people annually (United Nations, Department of Economic and Social Affairs, 2019). Thus, population is projected to grow by just over than one billion people over the next 13 years and it is estimated that in 2050 the number of its inhabitants will grow to almost 10 billion (United Nations, Department of Economic and Social Affairs, 2019).

The world population growth has also coupled with an increase in food demand by developing countries (FAO, 2017; United Nations, Department of Economic and Social Affairs, 2019; Vaccari et al., 2018). This has led to a rise of food production and consumption; in particular, meat production is progressively increasing (FAO, 2017; Vaccari et al., 2018), with 210 million tons produced in Europe in 2014 (FAO, 2017).

The global growing food consumption translates into an increment of effluents and waste production (FAO, 2017; Jadhav et al., 2017; Nghiem et al., 2017). As described by the Eurostat report (Eurostat - Statistic explained, n.d.), the total amount of wastes generated by all economic activities and households in the European Union, reached a production peak of 2,503 million tons in 2014. Nevertheless, the trend of total wastes production has been quite stable from 2014 to 2017 and the waste amount (excluding major mineral waste) generated by agriculture, forestry and fishing has fallen by 68.7% (Eurostat - Statistic explained, n.d.).

Another issue that arises along with the increasing food supply is the growth of global demand for fertilizers (FAO, 2017; IFA, 2014), specifically nitrogen (N), phosphate (P) and potash (K). In the following years the fertilizer production is expected to reach 201.66 million tonnes by the end of 2020 (FAO, 2017), with an average annual increase of 1.9 %. These are alarming data, considering not only the steady increase in demand for fertilizers but also the potentially pollutant nature of nitrogen and

phosphorus (FAO, 2017). Taking this into account, in the last decade, the common purpose has been to limit the nitrogen damage due to livestock effluents pollution (Nitrates Directive 91/676/EEC), in consideration of the fact that animal sewages contain the highest amounts of total nitrogen and phosphorus (Fleming and Ford, 2001; Vaccari et al., 2018). Specifically, one human daily produces 9.1 g of total N and 1.8 g of total P, while a dairy cow produces respectively 260 g and 55 g a day and a feeder pig 27 g and 9.4 g (Fleming and Ford, 2001). In summary, 1,000 humans generate as much total nitrogen as 340 pigs or 40 cows and as much total P as 190 pigs or 30 cows (Fleming and Ford, 2001). Unfortunately, the nitrogen targeted measures of the European Union (Nitrates Directive 91/676/EEC) are insufficient for dealing with the land disposal of manure (Szogi et al., 2015; Szögi et al., 2015). Farmers, in fact, apply manure following N-based criteria, but the unbalanced nitrogen-phosphorus ratio for crop production leads to the overloading of phosphorus in soils (Evanylo et al., 2008; Szögi et al., 2015; Zhang et al., 2003). Manure phosphorus concentration is higher than the amount removed in harvested crops and while nitrogen gets adsorbed by plants, phosphorus accumulation increases the risks of transfer from soil to water, finally causing its pollution (Szogi et al., 2015; Zhang et al., 2003).

Global human activity discharges annually 1.62 million tons of P into the major freshwater pools on Earth (Mekonnen and Hoekstra, 2018; Seitzinger et al., 2010), surpassing the planet assimilation capability for the phosphorus excesses in water bodies (Mekonnen and Hoekstra, 2018; Vaccari et al., 2018). Reports in 2018 referred that the phosphorus massive input in freshwater bodies exceeded the assimilation capacity on the 38% of the land surface (Mekonnen and Hoekstra, 2018). This is a worrying report since the massive input of phosphorus into natural water bodies is the main cause of eutrophication, which affects the survival of many aquatic species (Ashley et al., 2011; Dyhrman et al., 2007). Eutrophication occurs when the nutrients in water exceed the amount required for normal growth and the proliferation of algae generates a cover at the top of the water, preventing sunlight from reaching aquatic plants (Ashley et al., 2011; Seitzinger et al., 2010). This causes their death, leading to a decrease in water oxygen levels and consequently causing the death of all the aquatic organisms (Seitzinger et al.,

2010). In order to overcome this problem it has been taken several measures, such as the improvement of the Urban Wastewater Treatment Directive 91/271 (UWWTD) (Council of the European Communities, 1991) and the Regulation n. 259/2012 (Parliament, 2012), which have led to a development in the European wastewater treatment system to adapt to new discharge regulations (Jaffer et al., 2002).

The P pollution problem runs alongside the rising demand for phosphate mineral fertilizers. To meet the food and industries demand, phosphorus is obtained from phosphate rocks, a limited and non-renewable source which is going to decrease from 2050 onwards (Ashley et al., 2011; Kataki et al., 2016a; Vaccari et al., 2018). Moreover, due to the current economic and technological conditions the majority of this world phosphate reserves, estimated to be about 300 billion tons (U.S. Geological Survey, n.d.), is not available for extraction. Although wide deposits have been found in the oceanic continental shelves (Vaccari et al., 2018), the use of these deposits is reasonably unaffordable. Currently, the major quantities of phosphorus are mined in China while Morocco detains the 74% of the available global deposits of phosphate rock and South Africa exports the biggest quantity (Desmidt et al., 2015; Kataki et al., 2016a; Nakakubo et al., 2012; Sørensen et al., 2015). Europe is the region most dependent on imports which are the 86% of its total demand due to a very low local phosphorus production (IFA, 2014). Therefore, the geopolitical situation can have a significant impact on the P availability and price (Guedes et al., 2014). The increasing perception of a global phosphorus crisis could therefore determine serious international tensions due both to the Earth's reserves distribution and their control and to the world population growth (Vaccari et al., 2018).

In consideration of these questions related to the phosphorus issue, the strategies and technologies aimed to recover this element represent the resolution to respond both to the forthcoming collapse of the fertilizer's supply and to the rising eutrophication problem. The most promising technologies to overcome these concerns are the P-recovery processes which can achieve phosphorus-free effluents from wastewater treatment plants (WWTPs) and which focus on by-products reusable for other

purposes. Nowadays, these processes are mostly applied to urban and industrial sewage, while there are few approaches available for treating livestock manure due to the lack of suitable markets for processed residues and the ready availability of low-cost alternatives (Vaccari et al., 2018). Moreover, livestock manure has a high total solid (TS) content (TS >5% DM) which seems to be one of the main limitations for the recovery of P from the influent solution (Tarragó et al., 2018; Yetilmezsoy et al., 2017). While the fields needs further studies, other methods use several metal salts such as iron ( $\text{FeSO}_4$ ,  $\text{FeCl}_3$ ) and aluminum compounds (alum,  $\text{Al}(\text{OH})_3$ ) to obtain a rapid and effective phosphate precipitation (Cordell et al., 2011). However, the limitations arise from the toxicity of the Al-rich resulting products, which can be hardly reused in agriculture (Cordell et al., 2011). Another example is the use of lime products ( $\text{CaO}$ ,  $\text{Ca}(\text{OH})_2$ ) for soluble phosphorus precipitation as Ca or Mg phosphates in alkaline conditions (Cieřlik and Konieczka, 2017). The final products may be employed as slow-release fertilizers; however, the method requires high amounts of lime and could involve high chemical inputs and handling costs but also excessive slurry generation (Cieřlik and Konieczka, 2017).

## **1.2 Research context and objectives**

This study focuses on one of the alternative methods for phosphorus recovery from the digested sludge. In the specific, phosphorus can be recovered from waste streams by the crystallization of struvite ( $\text{MgNH}_4\text{PO}_4 \cdot 6\text{H}_2\text{O}$ ), which is an effective slow-release fertilizer and it offers many advantages versus conventional fertilizers, such as low leach rates and slowly release of nutrients. Many technological approaches are being developed to enhance struvite precipitation but few of them are suitable for livestock effluents, which are characterized by high solids concentration (3-4 % TS) that affect struvite crystallization rate. The struvite crystallizers technology had been developed in different prototypes and put into production successfully abroad.

This study aims to elucidate the effect of solids (3-4 % TS) on struvite formation in a complex matrix, such as animal slurries and digestates. Special attention is given to identifying the role of solids in struvite nucleation and growth, and its impact on the quality of the product recovered.



## **2. LITERATURE REVIEW: LOW-COST STRATEGIES FOR PHOSPHORUS REMOVAL FROM ANIMAL MANURE**

### **2.1 Introduction**

This literature review considers the low-cost techniques which remove and recover P from livestock wastes, evaluating their applicability to phosphorus sustainability. Special attention is given to the use of by-products in P recovery and to the induction of struvite precipitation in crystallizer prototypes.

In farms, phosphorus recovery from animal manure is largely limited by logistical and economic barriers, especially in small units where equipment and input costs quickly become prohibitive (Szogi et al., 2015). For zootechnical wastewaters, solid-liquid separation is commonly the first step, removing the P bounded to particles, solids and organic matter, which may affect following treatments (Szogi et al., 2015; Tambone et al., 2017). There are several technologies for P recovery and fertilizer production from animal slurries and some of them can achieve efficient P inorganic removal while keeping the operations relatively low-cost, i.e. chemical precipitation, biochar production and electrocoagulation (Tab. 1) (Fig. 1) (Hu, 2016; Kiran et al., 2017; Schoumans et al., 2017; Yetilmezsoy et al., 2017).

Table 1: Summary of recent low-cost technologies for P recovery from livestock effluents.

Recovery and removal technologies	Substrate	Objective	Advantages	Disadvantages	References
<b>Precipitation</b>					
Struvite (MgNH <sub>4</sub> PO <sub>4</sub> )	Urine Sewage sludge Synthetic wastewater Synthetic wastewater - Swine digestate -	Fertilizer production, P removal	Low cost; Re-use of byproducts (seawater bittern as Mg source); Fertilizer production.	Zonal availability of seawater bittern	<i>Etter et al., 2011;</i> <i>Cièslik et al., 2017;</i> <i>Crutchik et al., 2017;</i> <i>Yetilmezsoy et al., 2017;</i> <i>Vaccari et al., 2018;</i> <i>Tarragò et al., 2018;</i> <i>Li et al., 2019.</i>
Calcium phosphates (Ca <sub>5</sub> (PO <sub>4</sub> ) <sub>3</sub> (OH), CaNH <sub>4</sub> PO <sub>4</sub> ·H <sub>2</sub> O)	Swine manure Anaerobic supernatant Swine slurry -	Fertilizer production, P removal	Large scale plants; High availability feedstock; Fertilizers production	Chemical input and related costs; Excessive sludge generation at high dosage	<i>Cordell et al., 2011;</i> <i>Makara and Kowalski, 2015;</i> <i>Dai et al., 2017;</i> <i>Schoumans et al., 2017;</i> <i>Vaccari et al., 2018.</i>
<b>Electrocoagulation</b>					
Electrodes made by low carbon steel, grey cast iron, flat bar for industrial use, aluminum, magnesium.	Municipal wastewater Swine wastewater Synthetic wastewater Swine manure	P removal and recovery	Low-cost; Simple set-up	Good as a pretreatment; Set-up from small to big scale for livestock effluent	<i>Stafford et al., 2014;</i> <i>Mores et al., 2016;</i> <i>Omwene et al., 2018;</i> <i>Zhang et al., 2018.</i>
<b>Biochar production</b>					
Pyrolysis of organic matter (biomass, residues, manures, wastes, etc.)	Swine manure Cow manure Swine slurry Swine manure	Waste recovery and energy production	P-rich ashes; Amending properties product	Needed further sperimentations	<i>Azuara et al., 2013;</i> <i>Kiran et al., 2017;</i> <i>Schoumans et al., 2017;</i> <i>Szögi et al., 2018</i>

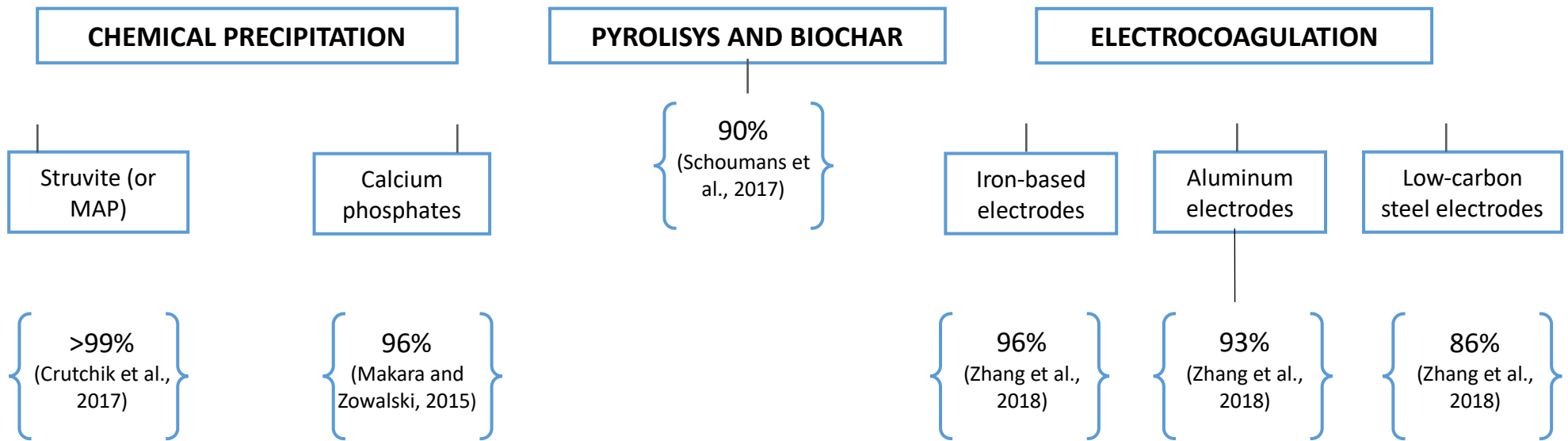


**Fig. 1** Efficiencies of the described P recovery approaches

## 2.2 Chemical precipitation

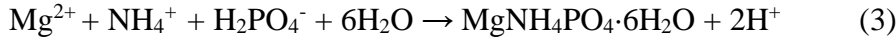
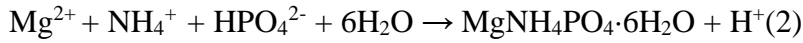
Chemical precipitation, also called crystallization, is a process that occurs spontaneously when phosphate concentration reaches the optimum for achieving thermodynamic super-saturation (Doyle et al., 2003; Rittmann et al., 2011). Precipitation usually is induced by the addition of a metal ion, such as magnesium ( $Mg^{2+}$ ), aluminum ( $Al^{3+}$ ), ferric iron ( $Fe^{3+}$ ) or calcium ( $Ca^{2+}$ ) (He et al., 2007). The salts precipitate as insoluble hydroxides and are then subjected to co-precipitation and adsorption to the metal hydroxides (Vaccari et al., 2018). The choice between the different metal salts normally used to start the precipitation affects the potential of the P removed to be reused for agricultural and industrial applications (De-Bashan and Bashan, 2004; Rittmann et al., 2011; Zhang et al., 2018).

### 2.2.1 Magnesium-based precipitation

The use of magnesium ( $MgO$ ,  $Mg(OH)_2$  and  $MgCl_2$ ) determine soluble phosphorus precipitation as different Ca and Mg phosphates at alkaline conditions if provided with the magnesium and calcium surplus necessary for P abatement (Burns et al., 2003; Kataki et al., 2016b). The final products are relatively insoluble but may be used as slow-release fertilizers (Rittmann et al., 2011).

The most promising compound for P recovery is struvite ( $MgNH_4PO_4 \cdot 6H_2O$ ), which precipitates spontaneously once phosphates reach 100-200 mg L<sup>-1</sup>. Struvite is formed from the combination of magnesium, ammonium, and phosphate at a stoichiometric molar ratio of  $Mg^{2+}: NH_4^+-N: PO_4^{3-}-P = 1:1:1$  (Yetilmezsoy et al., 2017).

The process of struvite crystallization is described in the Eq.1-2-3, whereas the reaction of  $HPO_4^{2-}$  is the dominant in the pH range of struvite precipitation (pH 7–11) (Jaffer et al., 2002).



Supersaturation is considered to be the engine in struvite formation and in all crystallization processes since it considerably affects the induction time of crystallization and the crystal growth rate (Shih and Yan, 2016). The struvite developing induction time is inversely proportional to the supersaturation of the solution (Li et al., 2019). The struvite supersaturation can be described through the saturation index (SI) shown in Eq.4 (Stolzenburg et al., 2014).

$$\text{SI} = \log ((a_{\text{Mg}^{2+}} \cdot a_{\text{NH}_4^+} \cdot a_{\text{PO}_4^{3-}})/K_{\text{struvite}}) \quad (4)$$

where  $K_{\text{struvite}}$  is the struvite solubility product while  $a_i$  is the activity of species' ion.

The dynamics of struvite formation are illustrated in Fig. 2, where line 0 represents the solubility curve of struvite and line between  $a$  and  $b$  represents the supersaturation curve. The unstable supersaturated area (point  $a$ ) is where crystal nucleation takes place, while is in the metastable supersaturated area (point  $b$ ) is favorable for the crystals growth. In the unsaturated stable area below line AB (point  $c$ ) the SI is below 0, which is not favorable for the crystals nucleation (Fang et al., 2016).

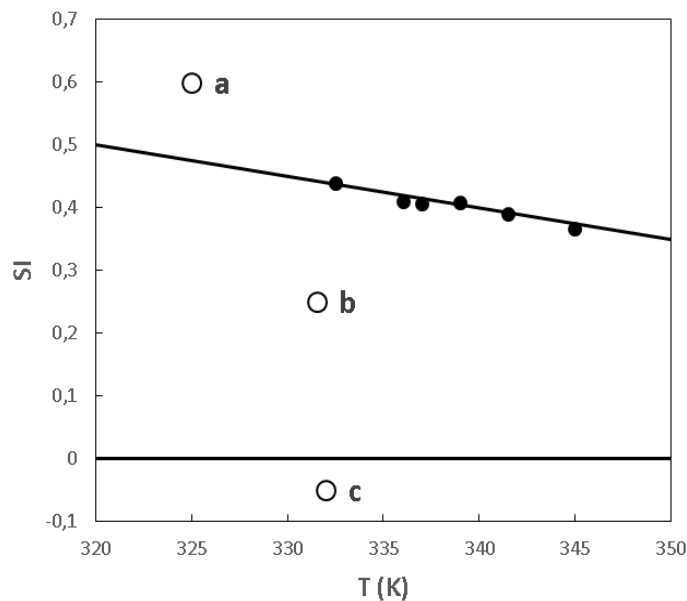


**Fig. 2** Relationship between the degree of supersaturation of struvite solution and struvite crystallization (Data source: Fang et al., 2016)

Struvite simultaneously recovers both nitrogen and phosphorus and has multiple commercial uses, including fertilizers and animal feed, cosmetics and detergents, fire-resistant panels and cement (De-Bashan and Bashan, 2004; Gaterell et al., 2000). It has excellent fertilizing properties and the low aqueous solubility of its crystals allows a prolonged duration of its fertilizing action over time (Li et al., 2019).

Many technological approaches are being developed to enhance struvite precipitation but few of them are suitable for livestock effluents, which are characterized by high suspended-solids concentration (3 g TSS L<sup>-1</sup>) that affect the struvite crystallization rate (Li et al., 2019). The struvite crystallizer technology has been developed in different prototypes (Tab. 2) and put into production successfully abroad (Crutchik et al., 2018; Desmidt et al., 2015; Le Corre et al., 2009, 2005; Li et al., 2019; Marchi et al., 2015; Rahaman et al., 2014; Tarragó et al., 2016; Zhang et al., 2018). The Tarragó et al. (Tarragó et al., 2018) prototype, in evaluating struvite removal, was able to reduce the influent concentration in

pig slurries from  $\sim 370 \text{ mg PO}_4^{3-} \text{ L}^{-1}$  to  $\sim 15 \text{ mg PO}_4^{3-} \text{ L}^{-1}$  with  $>95\%$  recovery efficiency. Moreover, the outcomes showed that solids ( $1\text{-}3 \text{ g TSS L}^{-1}$ ) didn't affect struvite formation, since they have a significant role in struvite crystallization, acting as surface for crystals nucleation (Tarragó et al., 2018).

Struvite technology is close to commercialization, although the costs of chemical inputs are very high when  $\text{MgCl}_2$  or another Mg source (magnesia or magnesite, wood ashes or MgO production by-products) are used in the process (Cieřlik and Konieczka, 2017; Jordaan et al., 2009; Kataki et al., 2016a; Pastor et al., 2008). However, a promising strategy for P removal is the use of seawater bittern (SWB), which is a by-product of sea salt production and a source of magnesium obtainable for free at the production site (Etter et al., 2011). Similarly to spontaneous struvite formation, this is the cheapest strategy if it is locally produced (Etter et al., 2011) and the most efficient, allowing operators to remove from wastewaters 83% of the ammonia and 99% of phosphorus at a pH of 10.5 (Crutchik et al., 2018; Shin and Lee, 1998). The high potential of this strategy for P removal and struvite recovery from livestock effluents will be analyzed in detail later in this review.

Table 2: Summary of reactor used for struvite crystallization and their efficiency

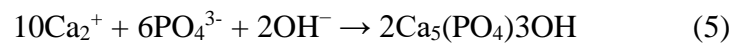
<b>Crystallizer</b>	<b>Substrate</b>	<b>Efficiency (% P recovery)</b>	<b>References</b>
Fluidized bed reactor (FBR)	Dewatered filtrate from anaerobic digestion	90%	Ishikawa et al., 2004; Ueno and Fujii, 2004; Guadie et al., 2014;
Bach test and pilot reactor (air-lift)	WWT's digested sludge	Pilot reactor:58-90%	Stumpf et al., 2008
Stirred tank reactor (reaction and settling zone)	Rejected liquors of different sludge treatments	70-90%	Martì et al., 2008; Li et al., 2019
Short-long column	WWT's digestate	70-90%	Bergmans, 2011
Air-lift crystallizer	Synthetic saturated solution	n.d.	Soare et al., 2012
U-shape reactor	Anaerobic digested effluents (swine)	n.d.	Zhang et al., 2014 Li et al., 2019
Air-lift reactor with a settler	Synthetic wastewater	>95%	Tarragò et al., 2016
Semi-CSTR	Swine	n.d.	Romero-Güiza et al., 2014; Li et al., 2019
Completely stirred tank reactor (CSTR)	Synthetic wastewater	84-87 %	Kuglarz et al., 2015; Crutchik et al., 2017; Liu et al., 2019



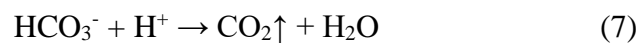
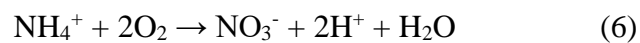
### 2.2.2 Calcium-Based Precipitation

In animal slurries, phosphorus may be initially released as  $\text{H}_2\text{PO}^-$ ,  $\text{HPO}^{2-}$  and/or  $\text{PO}^{3-}$  by lowering the pH and can be subsequently recovered by the addition of an alkaline source (e.g. calcite ( $\text{CaCO}_3$ ), hydrated lime ( $\text{Ca(OH)}_2$ ), bone charcoal etc.), forcing precipitation of a Ca-P. The product can finally be removed from the solution by filtering the suspension (Makara and Kowalski, 2015; Schoumans et al., 2017, 2010). This leads to a relatively small volume of precipitates which are highly concentrated in phosphorus and which can be easily used as a secondary resource of P fertilizer (Desmidt et al., 2015; Schoumans et al., 2017).

The use of calcium compound for P removal determines first the precipitation of Ca phosphate minerals as hydroxyapatite, brushite, monetite etc. The most widespread phosphate mineral is hydroxyapatite ( $\text{Ca}_5(\text{PO}_4)_3\text{OH}$ ), which formation is described in Eq. 5 b (Vanotti et al., 2003).



The high buffering capacity of liquid manure affects P precipitation in livestock effluents when alkaline compounds such as calcium hydroxide ( $\text{Ca(OH)}_2$ ) are used (Vanotti and Szogi, 2009). The pre-nitrification step could solve this problem (Eq.6-7), reducing the bicarbonate alkalinity and the concentration of  $\text{NH}_4^+$  (Vanotti et al., 2003).



Hydrated lime ( $\text{Ca(OH)}_2$ ) or the  $\text{Ca(OH)}_2$  and  $\text{Mg(OH)}_2$  combination are low-cost products (ICIS, 2018) which allow both the pH increase and the calcium addition. They also have been shown to be valuable in simple reactor tests for P precipitation from wastewaters (Desmidt et al., 2015; Vanotti and Szogi, 2009).

This calcium phosphate removal process may also be used to remove P in animal waste treatment systems both with and without anaerobic lagoons (Vanotti and Szogi, 2009). Vanotti and Szogi (2009) also reported that this technology (pilot scale) obtained the 95–98% of P removal as a phosphate from the anaerobic lagoons streams. In systems without a lagoon, an initial solid-liquid separation process removed most of the carbon compounds from raw liquid manure (Vanotti and Szogi, 2009). Once separated, the wastewater is both treated with nitrification and soluble P removal. In the latest improved methods, the P recovery process became more efficient, reducing equipment needs and chemicals with the introduction of a combined solid-liquid separation (Schoumans et al., 2014).

Although the use of lime it has been reported to determine the 95% of removal efficiency using animal manure, the necessity of high amount of this Ca mineral may result both in high chemical input and excessive sludge production and costs (Schoumans et al., 2014).

### **2.3 Electrocoagulation**

Electrocoagulation (EC) is an effective low-cost method for phosphorus (Nguyen et al., 2014; Ozyonar and Karagozoglu, 2011; Stafford et al., 2014; Tchamango et al., 2010) and solids removal (Hall and Abell, 2006; Hutnan et al., 2006) from several types of wastewater, such as synthetic wastewater (Attour et al., 2014; Bouamra et al., 2012; Inan and Alaydin, 2014), textile industries wastewaters (Chavan and Arega, 2018) and livestock effluents etc. (Zhang et al., 2018).

The EC process applies electricity to electrodes (usually aluminum or iron) immersed in the solution to be treated and connected externally to a direct current power supply (Fig. 3) (Symonds et al., 2015). The anode oxidation of metal electrodes releases metal ions that can work as coagulants, binding phosphate and enhancing the suspension of particles (Hu, 2016). In particular, during EC the coagulating ions are generated continuously by electrochemical dissolution of the sacrificial anode (Hakizimana et al., 2017). These ions spontaneously undergo hydrolysis in water forming different coagulant species including metallic hydroxide precipitates, which eliminate contaminants by adsorption or settling (Hakizimana et

al., 2017). The floc formation (as a result of the coagulation process) is characterized by the presence of metal hydroxo complexes in larger agglomerates, which in wastewaters can be treated by using physical separation process, such as screw press or filtration, floating or gravitational sedimentation (Stafford et al., 2014; Zhang et al., 2018).

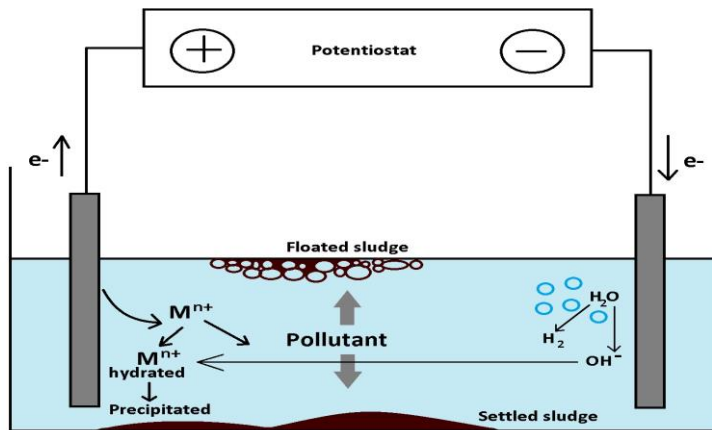


**Fig. 3** Simple electrocoagulation cell with reaction taking place during EC

Several electrode materials were tested as electrodes, e.g. lower steel carbon, aluminum, iron etc. Mores et al. (Mores et al., 2016) tested iron steel electrodes obtaining 96.3% of P removal, although this last result was reached by processing swine manure with an initial P concentration of  $70 \text{ mg L}^{-1}$ , which is much lower than the usual concentration of  $478\text{--}1756 \text{ mg L}^{-1}$  in swine manure (Hernandez and Schmitt, 2012). Zhang et al. (Zhang et al., 2018) evaluated low carbon steel electrodes and the results showed that EC method followed by 1 day spontaneous precipitation obtained the 72.6–86.3% of phosphorus removal from liquid swine manure.

Electrocoagulation could be considered as an alternative to chemical coagulation (Stafford et al., 2014; Zhang et al., 2018, 2016) since it offers some advantages: i. it has a simple set-up requirement and it can be automated; ii. it cuts the chemical cost by using cheaper materials (Omwene et al., 2018; Zhang et al., 2016); iii. gas bubbling promotes coagulation and the formation of bigger flocs; iv. pH is easily maintained because the cathode reaction consumes protons (Zhang et al., 2018, 2016). The findings of

these recent studies indicate that EC is a potential low-cost method for swine manure high-concentration P removal (Zhang et al., 2018).

## **2.4 Pyrolysis and Biochar**

There is a rising interest worldwide in the pyrolysis of biomass and organic residues (Azuara et al., 2013; Liu et al., 2018; Lů et al., 2013; Masebinu et al., 2019; Schoumans et al., 2010). Biochar production allows producers to employ the energy from biomass and organic wastes and it is a product which may have soil quality amending properties (Angst and Sohi, 2013; Bedussi et al., 2015; Cayuela et al., 2010; Foereid, 2015; Lehmann, 2009; Spokas and Reicosky, 2009; Steinbeiss et al., 2009). Moreover, due to its high nutritive value, biochar derived from animal manure contains essential plant nutrients and a high cation exchange capacity (CEC) (Kiran et al., 2017).

The organic matter (e.g. biomass, manures, residues and wastes) is heated inside a pyrolysis reactor, in an oxygen-free atmosphere, to a temperature between 350-700°C (under pressure). This produces biochar which is composed of carbon and inorganic material, including P-rich ashes (Fig. 4). The pyrolysis also produces a gaseous fraction (methane, hydrogen, carbon monoxide, carbon dioxides, etc.) and a liquid fraction consisting of tar and pyrolytic oil (Azuara et al., 2013; Schoumans et al., 2010).

Schoumans et al. (Schoumans et al., 2014) produced biochar from pig, poultry and cattle manure, and tested for its soil improvement potential. The results showed that the soil phosphorus availability increased considerably, suggesting that the biochar-derived phosphorus provided the plant-available phosphorus in the soil. Further testing is needed on potential biochar applications, as well as a general evaluation of the pyrolysis of solid manures.

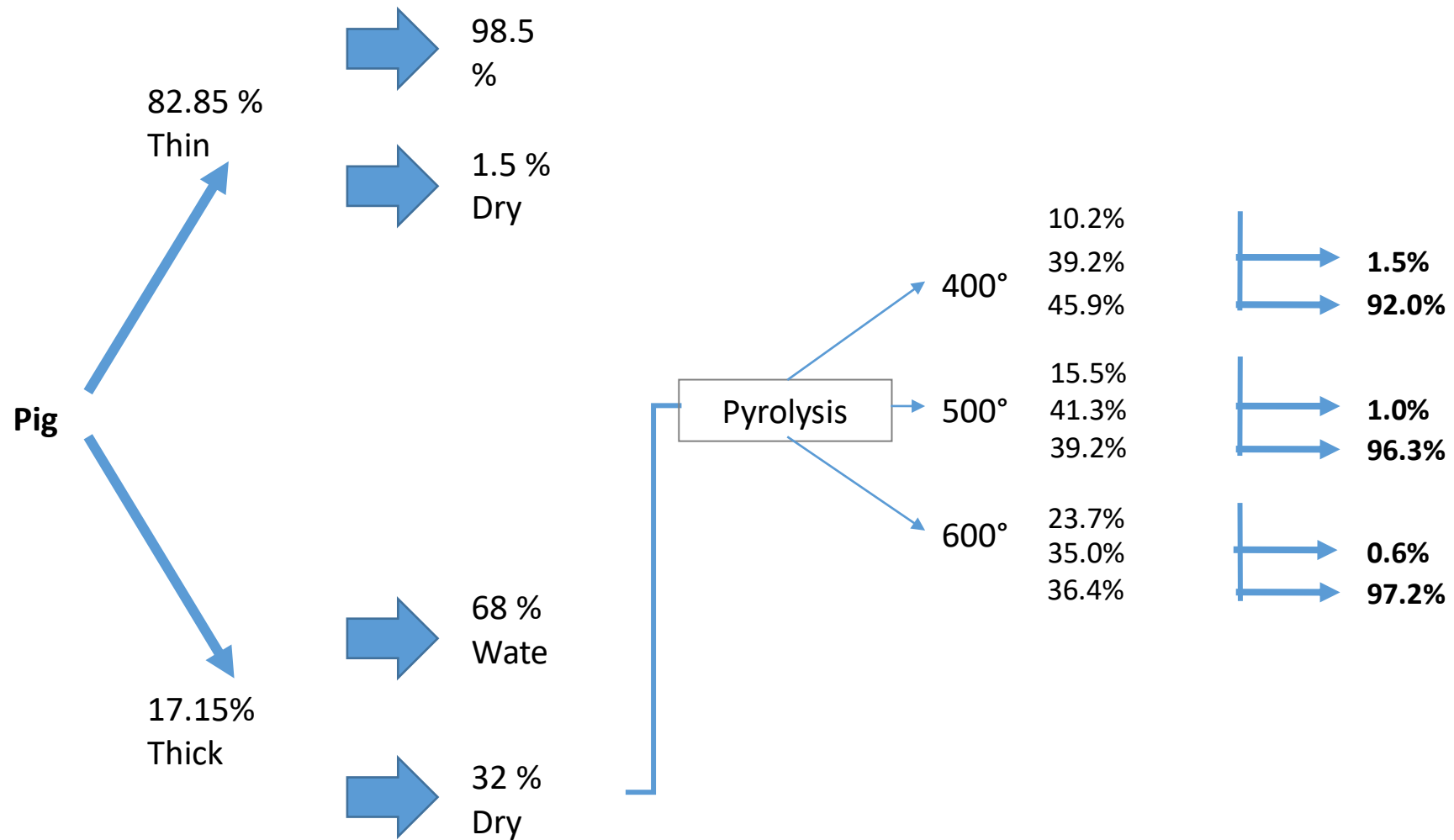


**Fig. 4** Distribution of products in pig manure pyrolysis and phosphorus mass balance (Data source: Azuara et al., 2013)

## 2.5 Struvite crystallization for P recovery from by-products

As described above, chemical precipitation, electrocoagulation (EC) and biochar production differ, with some advantages and disadvantages (Tab. 1). In particular, calcium phosphates precipitation is already applied at the large-scale (Schoumans et al., 2017), but it still needs massive chemical input which leads to an excessive sludge generation (Schoumans et al., 2017). Egle et al. (Egle et al., 2016) estimated that the total cost for a Ca-based crystallization process is about 1.5 € kg P<sup>-1</sup> including profit (with wastewater as treated effluent), while for the struvite crystallization the total cost is much lower, estimated at 0.01-0.22 € kg struvite<sup>-1</sup> (about 0.6 € kg P<sup>-1</sup>) including profit (using treated seawater as the Mg source) (Quist-Jensen et al., 2016). Biochar production also has higher expenses compared to struvite production: Azuara et al. (Azuara et al., 2013) estimated that the pyrolysis process for P removal from pig manure had approximately a total cost of 3 € kg P<sup>-1</sup> (Tab. 4). Finally, considering that EC is a newly emerged, potentially valuable technology there are some difficulties in estimating the production costs for a pilot-scale plant due to the low number of published works on the topic. The only available data were reported by Hu et al. (Hu, 2016) referring to an EC pilot-scale plant treating 100 L day<sup>-1</sup> of deep pit swine manure. According to the total cost reported, it was possible to estimate a recovery cost of 61.7 € kg P<sup>-1</sup>. As discussed before (Section 2), EC is a promising technology in livestock effluent treatment and the high recovery cost calculated here may be reduced in the near future by employing cheaper and re-usable materials.

A comparison of the energy consumption for these processes is also necessary to appreciate the advantages of the struvite synthesis approach (Tab. 4). Nevertheless, there are different factors which could influence the energy consumption in P-recovery, such as the amount of material processed, reagents used or the scale of the process considered (laboratory test, pilot or full-scale plant). Moreover, the energetic balance data for these P-recovery processes are not easily accessible, thus the energy analysis performed in this work will consider only struvite crystallization and the EC technologies.

Schoumans et al. (Schoumans et al., 2017) reported that a full-scale plant for the production of struvite from livestock effluents consumes 157 kWh for the treatment of 100,000 ton of digestate. The available data on the electrocoagulation process consumption refer to an EC pilot-scale plant, which utilizes about 0.453 kWh in processing 10 kg of manure (Hu, 2016). Although it is difficult to compare data from such different scale processes, it could be approximately estimated that the energy consumption for the treatment of 10 kg of digestate by a full-scale crystallization plant is  $1.6 \cdot 10^{-5}$  kWh (Hu, 2016). Therefore, the energy required by crystallization is four orders of magnitude lower than the energy spent in EC process and even if the calculation is affected by a standard deviation of two orders of magnitude (due to the different process scales), we can realistically affirm that the energy normally consumed by the crystallization process is far lower than the energy consumed by electrocoagulation.

Data discussed above indicate that among P recovery technologies, struvite crystallization has a great potential in the fertilizer market if the formation is promoted by using low-cost Mg sources and the recovery is controlled by crystallization technologies (Crutchik et al., 2018; Etter et al., 2011; Quist-Jensen et al., 2016; Tarragó et al., 2018, 2016; Ueno and Fujii, 2001). Since in last years struvite crystallization has obtained more interest as a method for phosphorus and nitrogen recovery from animal slurries (Fukumoto et al., 2011; Wang et al., 2013; Wilsenach et al., 2007), we will now describe in more detail the struvite formation and potential.

Struvite is a slow-release fertilizer which offers many advantages compared to the other conventional products. Specifically, it could be used to manage nutrient release, reducing the nutrient loss (Li et al., 2019), it has low leach rates (Münch and Barr, 2001) and thus it may have a relevant use in grassland and forest, which need one fertilizer application in several years (Cerrillo et al., 2015; Rahaman et al., 2014). If a high dose of fertilizer is applied, there is no damage to growing plants (De-Bashan and Bashan, 2004) and it is also an alternative for crops which require magnesium (Gaterell et al., 2000; Li et al., 2019). Finally, using struvite as fertilizer, the P uptake by plants shows high efficiency (Johnston and Richards, 2003).

Struvite crystallization technologies also have a role in nitrogen removal and recovery (Li et al., 2019). Although ammonium removal through struvite crystallization technology is practicable, it is not cost-effective due to the magnesium and phosphate salts high costs (Li et al., 2019). To face this difficulty, the recovered struvite can be subjected to pyrolysis in alkali solutions for further ammonium removal (H. Huang et al., 2011; Huang et al., 2012; H. M. Huang et al., 2011; Kataki et al., 2016a, 2016b). For example, using landfill leachate has been observed the 96%  $\text{NH}_4^+$  removal under optimal conditions ( $\text{OH}^-$ :  $\text{NH}_4^+$  of 1:1, temperature of 90 °C and time of 2 h) (He et al., 2007). It was also reported the 87% of  $\text{NH}_4^+$  recovery for yeast industry anaerobic effluent, in ideal conditions of  $\text{OH}^-$ :  $\text{NH}_4^+$  ratio of 1.5:1, pH of 9 and temperature of 110 °C, during an interval of 3 hours (Uysal et al., 2010).

Furthermore, struvite recovery gives economic advantages. The spontaneous precipitation of struvite inside treatment plant pipes in fact, makes plant operating less efficient and costlier (the crystals must be broken by hand or dissolved with sulfuric acid) (Durrant et al., 1999; Stratful et al., 2004; Williams, 1999). The solution to this economic and efficiency problem could be the precipitation of struvite in a specific reactor, instead of allowing spontaneous formation. Technologies for struvite crystallization have recently improved and many types of reactors have been developed (Table 2) (Bergmans, 2011; Crutchik et al., 2018; Marchi et al., 2015; Pastor et al., 2008; Soare et al., 2012; Stumpf et al., 2008; Tarragó et al., 2018, 2016; Ueno and Fujii, 2001). The crystallizer performances are evaluated in terms of efficiency (P-recovery), heated retention time (HRT), minimum theoretical equivalent diameter (MTD), the struvite production rate (i.e. the amount of struvite produced in a fixed time), a very important reactor parameter for efficiency estimation (Li et al., 2019).

In an effort to develop a low-cost phosphate recovery technology, the attention has recently focused on seawater bittern use as the Mg additive for struvite synthesis. Magnesium is the second cation for abundance in seawater (Mg content-1,300  $\text{mg l}^{-1}$ ) coming from the Mg minerals erosion (Kumashiro et al., 2001; Shin and Lee, 1998). Seawater bittern is the salt suspension remaining after crystallization of NaCl from seawater and it is characterized by a high Mg content of 9,220–32,000  $\text{mg L}^{-1}$ . Bittern has



been demonstrated valuable for struvite precipitation in animal and municipal wastewater, urine, coke and landfill leachate (Etter et al., 2011; Lee et al., 2003; Li and Zhao, 2003; Shin and Lee, 1998). In particular, the tests reported a total  $\text{PO}_4^{3-}$  recovery of 99% on coke manufacturing wastewater (Shin and Lee, 1998), 94% of P removal in urine (Merino-Jimenez et al., 2017) and 76% in swine wastewater (Kataki et al., 2016a; Lee et al., 2003; Pepè Sciarria et al., 2018).

The real value of bittern in struvite synthesis is thus proved, but the growing interest in this resource is because of its high availability and low cost. In fact, the use of  $\text{MgCl}_2 \cdot 6\text{H}_2\text{O}$  or other magnesium salts, affects the costs and sustainability of the struvite synthesis process (Quist-Jensen et al., 2016). Economic evaluations (Etter et al., 2011; Quist-Jensen et al., 2016; Yetilmezsoy et al., 2017) of Mg sources normally used in the struvite crystallization process are reported in Tab. 3.

Table 3: Economic analysis of magnesium sources normally used in the struvite crystallization process

Common magnesium sources	Total cost (€)	References
Magnesium chloride hexahydrate: $\text{MgCl}_2 \cdot 6\text{H}_2\text{O}$	€ 656.25 $\text{ton}^{-1}$	Dalian Chem Imp.& Exp. Group Co., Ltd. (2016)
Magnesium sulfate heptahydrate: $\text{MgSO}_4 \cdot 7\text{H}_2\text{O}$	€ 473.5 $\text{ton}^{-1}$	Shijiazhuang Xinlongwei Chemicals Co., Ltd. (2016)
Magnesium oxide: MgO	€ 612.5 $\text{ton}^{-1}$	Liaoning Metals & Minerals Enterprise Co., Ltd. (2016)

Seawater bittern has no cost of production since it is a waste brine remaining after salt ( $\text{NaCl}$ ) extraction from seawater. Nevertheless, the transportation costs from the coast might be an influence on the total expenses of the process. For example, Etter et al. (Etter et al., 2011) estimated the cost of SWB to be 0.22 €  $\text{kg struvite}^{-1}$  considering the transport to a pilot test site in Nepal located in an area far from the coast. Thus, SWB is very low-cost resource and even if in the potential areas of production the

magnesite is locally extracted, the price difference is small (the magnesite locally costs 0.12 € kg struvite<sup>-1</sup>) (Etter et al., 2011).

The use of a by-product in fertilizer synthesis is fundamental for an ecologically and socially sustainable economy. This makes the bittern solution attractive on the market (small and industrial production) and though its use is yet to be evaluated on a commercial scale, it may be an economic Mg source in regions neighbouring the sea (Crutchik et al., 2018; Etter et al., 2011; Lee et al., 2003; Li and Zhao, 2003; Matsumiya et al., 2000; Shin and Lee, 1998).

For example, the Dutch agricultural sector produces about 75 million kg P y<sup>-1</sup> as animal manure of which 25% cannot be applied to land in the Netherlands because of P application limits for agricultural land (Schoumans et al., 2017; Smit et al., 2015). This issue could be resolved by using the struvite crystallization approach (especially if enhanced by the SWB employment), considering that this low-cost technology could recover more than 90% of this discarded P (the equivalent of 17 million kg P y<sup>-1</sup>) in a highly usable product. Smit et al. (Smit et al., 2015) estimated that the import of P mineral fertilizer into the Netherlands is about 7 million kg P y<sup>-1</sup>. Thus, the recovery of P which cannot be applied as fertilizer in the Netherlands (i.e. 22% of the total 75 million kg P y<sup>-1</sup> produced) could potentially replace the demand for this mineral fertilizer, removing both the import costs and the issue of animal manure disposal.

In this context, another issue arises concerning the treatment of livestock effluents, since their high amounts of suspended solids (TS >5%) and organic matter may limit struvite crystallization (Havukainen et al., 2016). Nevertheless, this problem seems to be overcome since the action of solids in the entering stream has an influence on the nucleation stage (Tarragó et al., 2018), acting as the nuclei for struvite crystallization as demonstrated by Tarragó et al. (Tarragó et al., 2018).

Table 4: Summary of the analyzed technologies with respective P-recovery, economic and energetic balance.

Low-cost P-recovery technologies	Efficiency of the process (% P removed)	Total costs	Energy consumption*	References
Crystallization (Struvite)	>99 %	-	-	Crutchik et al., 2017;
	-	0.6 € kg P <sup>-1</sup>	-	Quist-Jensen et al., 2016;
	92%	-	1.6 · 10 <sup>-5</sup> kWh	Hu et al., 2016;;
	>99 %	-	-	Yetilmezsoy et al., 2017
Calcium phosphates precipitation	85 %	1.5 € kg P <sup>-1</sup>	-	Egle et al., 2016;
	86 %	-	-	Dai et al., 2017;
Electrocoagulation	98%	-	-	Fernandes et al., 2012
	96 %	61.7 € kg P <sup>-1</sup>	0.453 kWh	Hu et al., 2016;
	>99%	-	-	Omwene et al., 2018;
	86 %	-	-	Zhang et al., 2018;
Pyrolysis and Biochar	90 %	3 € kg P <sup>-1</sup>	-	Azuara et al., 2013;
	97%	-	-	Szögi et al., 2018

\*for the treatment of 10 kg of animal digestate.

### 3. MATERIALS AND METHODS

The experiments of this study were all conducted on the laboratory scale at the Gruppo Ricicla Labs, at the Agronomic and Environmental Sciences Department of the University of Milan. The material and methodologies used are described in detail in this chapter. The methodologies presentation is divided in paragraphs which follow the main experimentation phases: precipitation batch tests, crystallizer set-up description and efficiency calculations, type of analyses performed on influent solution and samples collected, agronomic tests set-up.

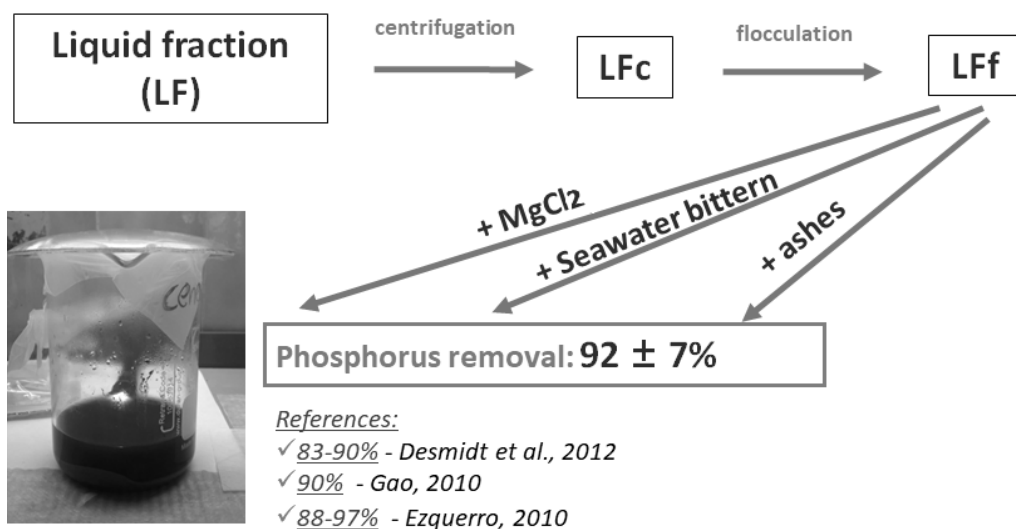
#### 3.1 Precipitation tests

As already explained, struvite precipitation requires specific parameters: presence of phosphorus and ammonium in a determined ratio, pH between 7.5 and 9.5, low-medium concentration of total solids (2-3 %). In a controlled environment (batch test) to speed up the struvite precipitation, magnesium source it is commonly added to the manure a magnesium source (e.g. magnesium chloride, mineral fertilizers). Thus, in this first step of the study were compared the efficiencies and advantages of:

- **MgCl<sub>2</sub> x 6H<sub>2</sub>O**, the common commercial salt;
- **Ashes** from a biomass (wood) combustion plant;
- **Seawater bittern (SWB)**, a by-product of halite evaporation in sea-salt processing rich in chloride, sulfate etc.

It was used the liquid fraction of 5 different digestates sampled in as many anaerobic digestion plants and obtained by a mechanical separation. The liquid fractions were centrifuged (6000 rpm) and flocculated using a commercial compound in order to reduce the total solids and organic matter contents. The samples were preliminary digested in microwave using HNO<sub>3</sub> and successively analyzed with ICP (Inductively coupled plasma mass spectrometry) for the determination of P and Mg total content (see paragraphs 3.4.2 - 3.4.5 for methodologies description). Moreover, the total

ammonium nitrogen was extracted using KCl 1N and determined by distillation and titration. These results allowed to calculate the optimum quantity for phosphorus precipitation from different sources (i.e. MgCl<sub>2</sub>, ashes and seawater bittern). Then, these sources were added to the liquid fractions in different concentrations and the pH was corrected until the optimum value for the struvite precipitation (pH 8.5). The samples were left overnight at room temperature, centrifuged and dried at 60°C. The dry sample compositions were analyzed by X-ray diffraction (XRD) (see paragraph 3.4.5), while the struvite crystals quality (purity, crystallization and precipitation dynamics) was evaluated by Scanning Electron Microscopy (SEM-EDS Oxford ISIS 300).



## 3.2 Crystallization system experimental set-up

### 3.2.1 Reactor working principles and procedures

A polymethyl methacrylate (PMMA) crystallizer was specifically designed to reproduce the optimal conditions for struvite precipitation (Fig. 5). In the specific, this prototype of air-lift reactor was differentiated in three zones: riser, clarifier and collector. The supersaturated condition of the riser zone ensured the struvite growth, enhanced by the recirculation and up-flow of small particles (centers of nucleation). The clarifier section consisted of a quiet zone in which these particles rise and

fall. In the collector, the nuclei settled once their settling velocity was higher than the up-flow velocity. The total volume of the crystallizer was 6.9 L and the hydraulic retention time (HRT) of 24 h. In the riser zone the influents were both the liquid fraction of digestate (fed continuously at 0.29 L h<sup>-1</sup>) and a seawater bittern solution as Mg source (fed continuously at 0.02 L h<sup>-1</sup>), added to allow struvite precipitation at different Mg<sup>2+</sup>/PO<sub>4</sub><sup>3-</sup> molar ratio for each test (see Chapter 4). In all the tests up-flow velocity and pH were the fixed parameters.

In the reactor the up-flow velocity (Eq.1) was kept constantly at 0.5 L min<sup>-1</sup> by means of a mass flow meter in order to match the critical settling velocity of the liquid particles.

$$\text{Up-flow velocity} = \text{Total flow/Section} \quad (\text{Eq. 1})$$

The operating pH in the reactor was constantly maintained between 8.5 and 9 with a NaOH 1M solution reduced using a control panel.

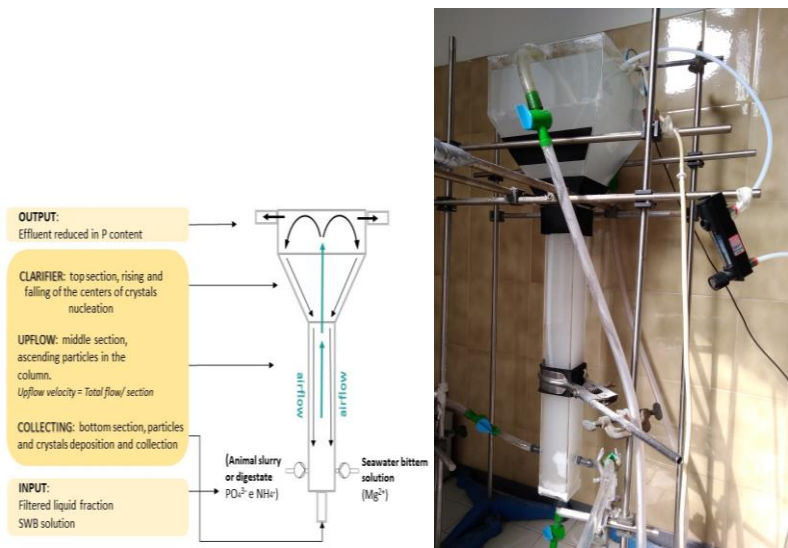


**Fig. 5** Crystallizer prototype set-up and operating details

The supersaturation (Sr) is the driving force for struvite formation (Tarragó et al., 2016). Sr was calculated based on the methodology followed by Bergmans (2011) (Eq. 2). The relative supersaturation is a function of the dimensionless supersaturation ratio (Sc), which depends both on

the analytical molar concentration ( $P_{so}$ ) and on the solution properties ( $P_{cs}$ ).  $P_{cs}$  is calculated from the minimum struvite solubility product ( $K_{so}$ ), the ionization fraction ( $a_i$ ) and the activity coefficients ( $c_i$ ) (Davies, 1962) of each struvite compound (Eq. 3). According to this, the solution is supersaturated for  $S_r > 0$  and undersaturated for  $S_r < 0$ .

$$S_r = S_c - 1 \quad (\text{Eq. 2})$$

$$S_c = (P_{so}/P_{cs})^{1/3} \quad (\text{Eq. 3})$$

The experimentation started with three tests in continuous using swine manure liquid fraction, to assess the best operating condition in terms of  $Mg^{2+}/PO_4^{3-}$  molar ratio and TS content (Test 1-3) and also using the literature information existent (Fernandes et al., 2012; Li et al., 2019; Marchi et al., 2015; Tarragó et al., 2018, 2016; Vanotti and Szogi, 2009). First three tests were carried out at the molar ratio  $Mg^{2+}/PO_4^{3-}$  of 1.8:1, 2:1 and 3:1 with a total solid content of 3.3%. Based on these first three test results, Test 4-5 verify the possibility to work with raw swine digested manure (TS 4.5%). Results and considerations of this first step experimentation merged in a second phase of the study, in which was changed the working substrate. In particular, was used cattle digested manure for the Test 6 and OFMSW digested effluent in Test 7, while the  $Mg^{2+}/PO_4^{3-}$  molar ratio and TS content were fixed to the previous test working values.

Struvite particles settled in the collector zone of the crystallizer were daily recovered together with the effluent wastewater.

### 3.2.2 Influent solutions

In the Test 1-5 was used as substrate the liquid fraction of swine digestates separated by screw press, (Tab. 6) in order to study both the effect of SWB in the phosphorus removal (Test 1-3) and the effects of increasing solids concentration (Test 4-5). The substrates were changed in Test 6-7, in which were used the liquid fraction (non-filtered raw material) of cattle manure (Tab. 7) and

OFMSW (Organic Fraction of Municipal Solid Wastes) digestate (Tab. 78 as substrate for struvite crystallization, to evaluate the crystallizer performances working with different type of influent solutions and high TS contents.

The magnesium source used for struvite precipitation was the “seawater bittern” (SWB), which is a by-product of sea salt processing mainly composed by magnesium chloride (>95%) and a low-cost material. Thus, the manure liquid fraction was filtered accordingly to achieve the desired concentration of solids and the influent SWB magnesium solution was dosed in order to get the specific  $\text{Mg}^{2+}/\text{PO}_4^{3-}$  molar ratio.

### **3.3 DM, TKN and total $\text{P}_2\text{O}_5$ breakdown calculations**

Separation efficiency between the solid (% SF) and liquid fraction (% LF) on fresh weight (FW) was calculated using the Eq. 4 (Tambone et al., 2017).

$$y = (5E^{-6} x^{2.3878}) \times 100$$

where y represents the solid fraction (% FW) and x the dry matter content of the considered digestate ( $\text{g kg}^{-1}$  FW). The liquid fraction (% FW) was calculated as:  $100 - \text{SF}$  (Tab. 5-7). The results were processed by ANOVA using the Tukey test to compare means. All statistical analyses were carried out using SPSS statistical software (version 16) (SPSS, Chicago, IL).

### **3.4 Samples characterization**

The influent solution of each test as the collector samples and batch tests were characterized using different methods as described in this paragraph, to assess the test performances and results.



#### *3.4.1 Total Kjeldhal Nitrogen (TKN) analyses*

TKN value is a measure of ammonia ( $\text{NH}_3$ ), organic nitrogen and ammonium ( $\text{NH}_4^+$ ) contained in the sample and it's a fundamental parameter to determine for struvite crystallization process. The TKN analysis required a preliminary mineralization of the samples (fresh materials), in which were added 20 ml di  $\text{H}_2\text{SO}_4$ , copper oxide ( $\text{CuO}$ ) and selenium dioxide ( $\text{SeO}_2$ ) according to standard procedures (IRSA CNR, 1994). After 1 h of heating at 90 °C the samples were distilled using a Kjeldhall Distillation Unit K-350 and titrated to sulfuric acid according to IRSA CNR (1994) methodologies.

#### *3.4.2 Total Phosphorus ( $P_{\text{tot}}$ ) analyses*

The samples were previously microwave-digested using 10 ml of diluted (65%) nitric acid ( $\text{HNO}_3$ ). The total phosphorus content was then determined using the inductively coupled plasma-mass spectrometer (ICP-MS) in order to monitor the crystallizer efficiency and the P removal during the different tests.

#### *3.4.3 Total organic carbon (TOC)*

TOC was analyzed to observe the path of the organic fraction in the crystallization process and to characterize the final product (and possible fertilizer) collected in the different tests. According to standard procedures (ALPHA, 1992) for the oxidation of organic carbon was used a 2 N solution of potassium dichromate ( $\text{K}_2\text{Cr}_2\text{O}_7$ ), while sulfuric acid ( $\text{H}_2\text{SO}_4$ ) was suitable for inorganic carbon removal. Total organic carbon was determined by titration to sulfuric acid (ALPHA, 1992).

#### *3.4.4 Total solids (TS) determination*

Total solids analysis evaluated the particles path from the influent solution until the collector effluent, since they play an important role in struvite formation. According to standard procedures

(ALPHA, 1992) for TS determination, the samples (preliminary weighed) were dried at 103-105°C, then ignited at 550 °C in a muffle and the residues were finally weighed.

#### *3.4.5 Optical and X-ray diffraction analyses*

Microscopic analyses were performed on the collector and effluent samples to analyze the macro-differences within the two output flows, both to verify the crystals presence and to assess the formation dynamics and growth. X-ray diffraction analyses were performed to determine the crystal structure and thus the nature of the crystals previously observed with microscopic analyses. The sample preparation for both the analyses was the drying of the materials at 103-105 °C and the following crushing.

### **3.5 Agronomic experimentation groundwork**

#### *3.5.1 Fertilizing product characterization: P speciation*

The fertilizing properties of the crystallizer output flow were also tested, analyzing the availability of the struvite phosphorus inside the collector samples. These data were compared with the chemical characteristics of both poultry manure and inorganic fertilizer, in order to verify the differences in the P availability in the short, medium and long-time interval.

It was measured the total phosphorus inside these three fertilizers as described in paragraph 3.4.2 of this Chapter, while the available P was determined with extraction in NaHCO<sub>3</sub> and spectrophotometric analysis ( $\lambda=650$  nm), according to standard procedure (Olsen et al., 1954). Phosphorus fractionation was finally determined (on poultry manure, on the crystallizer's struvite and on mineral fertilizer) using the methodology as reported by Turner B.L. e Leytem A.B. (2004). Phosphorus fractionation was consequently evaluated also after the pot trials on *Brassica rapa chinensis* (see following paragraph 3.5.2 "Pot trials set-up") on the soils fertilized with the three different fertilizer types, to determine phosphorus solubility and availability.

### 3.5.2 Pot trials set-up

Twelve pot trials were settled-up to test the differences between the three fertilizers used and to assess the potential of the struvite collected during the different tests in the pilot plant (Tab. 5).

The tests were conducted in pots using *Brassica rapa chinensis* (Green rocket variety) grown under the same conditions monitored in a phytotron for 26 days, with an average temperature of 25 °C, 60% of moisture, 16 hours of light and 8 hours of dark.

The substrate for plant growth was an improving peaty soil (NUAVA FRESAN B 0-5 UNGURI 19/01/2015), with a low nutrient content (hypotrophic) both to minimize the interferences with the agronomic test and to allow an accurate dosage of the nutrients input. However, considering the low pH value of the soil chosen, CaCO<sub>3</sub> was added to the pot to raise the pH until the optimal value for *Brassica rapa chinensis* cultivation.

In the specific, for soil fertilization were used

- for 3 specimens: struvite (P), K<sub>2</sub>SO<sub>4</sub> (K), urea (N);
- for 3 specimens: poultry manure (N + P), K<sub>2</sub>SO<sub>4</sub> (K);
- for 3 specimens: mineral fertilizers as: urea (N), K<sub>2</sub>SO<sub>4</sub> (K), Ca(H<sub>2</sub>PO<sub>4</sub>)<sub>2</sub> (P);
- 3 specimens as blank test, with no fertilizers added.

Tab. 5 Fertilization plan for *Brassica rapa chinensis*.

	Fertilizer	Urea (g/pot)	K <sub>2</sub> SO <sub>4</sub> (g/pot)	Ca(H <sub>2</sub> PO <sub>4</sub> ) <sub>2</sub> (g/pot)	Poultry manure (g/pot)	Struvite (g/pot)
S1	Struvite	0,70	2,774	-	-	4,80
S2	Struvite	0,70	2,774	-	-	4,80
S2	Struvite	0,70	2,774	-	-	4,80
P1	Poultry manure	-	2,774	-	12,88	-
P2	Poultry manure	-	2,774	-	12,88	-
P3	Poultry manure	-	2,774	-	12,88	-
M1	Mineral	0,70	2,774	0,939	-	-
M2	Mineral	0,70	2,774	0,939	-	-
M3	Mineral	0,70	2,774	0,939	-	-
∅1	Blank	0	0	0	0	0
∅2	Blank	0	0	0	0	0
∅3	Blank	0	0	0	0	0

Pot trials were concluded with NP soil analyses (methodologies as indicated in § 3.3.1 and 3.3.2) after fertilizations to determine phosphorus availability and solubility.

Finally, chlorophyll A and B were measured according to standard procedures (Lorenzen, 1965; Strickland and Parsons, 1968), through extraction with acetone (C<sub>3</sub>H<sub>6</sub>O) and spectroscopic analysis (645 nm of wavelength for chlorophyll b and 663 nm for chlorophyll a).

## 4. RESULTS AND DISCUSSION

This chapter includes results of this study, comparison of these findings with literature information and a discussion on the different performances obtained. In a first step was identified the best magnesium source in terms of efficiency and quality of struvite recovered. In a second part of this chapter will be described the crystallizer performances obtained with different substrates (swine, cattle and OFMSW).

### 4.1 Batch tests results

The results show that the presence of magnesium is the limiting factor in the struvite precipitation. The following centrifugation and flocculation treatments aim to minimize the dry matter content and to maximize the phosphorus one. In fact, the centrifugation determines a significant decrease of the dry matter percentage. The addition of the different Mg sources shows significant variations in quality and quantity of the struvite precipitation.

SEM analyses showed that in the spontaneous precipitation the struvite crystals were aggregated in a matrix of various salts (Mg, Ca, Cl) and the formations were stratified (Fig. 7).

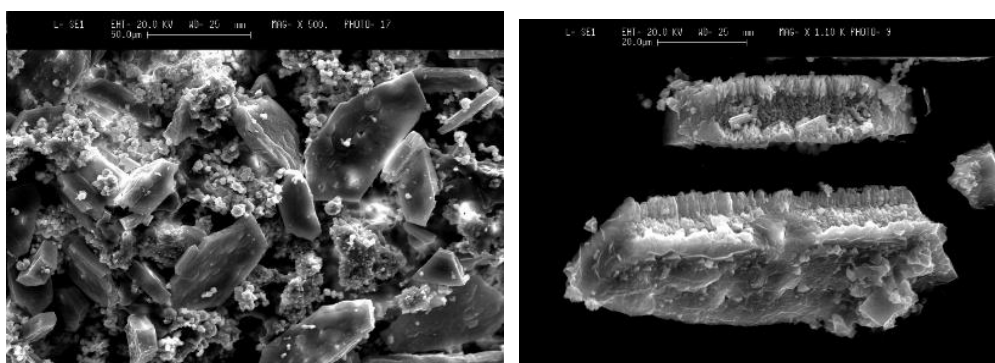


**Fig. 7** Struvite crystals recovered from spontaneous precipitation (left) and stratified structures in the crystals (right) (SEM photography).

In the extraction with ashes was noticed a few amounts of precipitated struvite and more aggregation between crystals and the salt matrix, in which there were also aluminum, silicon and iron (Fig. 8). The  $MgCl_2$  addition allowed a better precipitation, with struvite crystals containing less calcium and more phosphorus, magnesium and ammonium, even if there were still aggregated in the matrix of salt (Fig. 8).

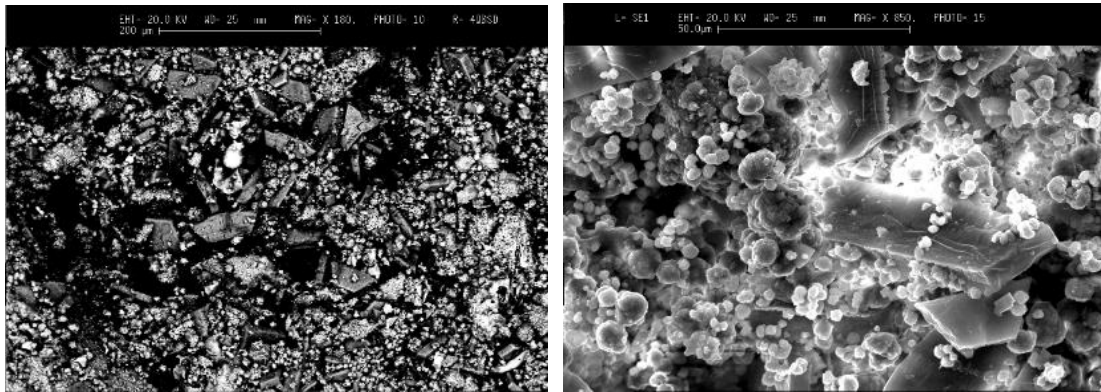


**Fig. 8** Ashes extraction at SEM photography (left); struvite crystals and salt matrix in  $MgCl_2$  extraction (right)

Finally, SWB extraction allowed a higher precipitation in comparison with the other Mg sources. The crystals observed were defined, separated and sometimes stuck in a carbonious matrix (Fig. 9). Moreover, crystals composition showed a minimum intrusion of other elements (Fig. 10). Considering these data, this the best treatment in terms of quantity and quality of precipitated struvite.

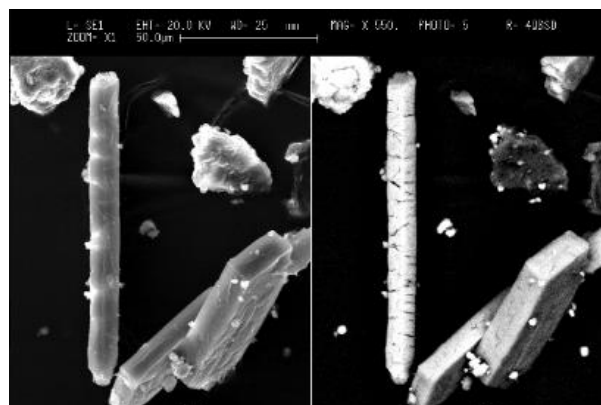


**Fig. 9** Struvite crystals in SWB extraction (SEM photography)

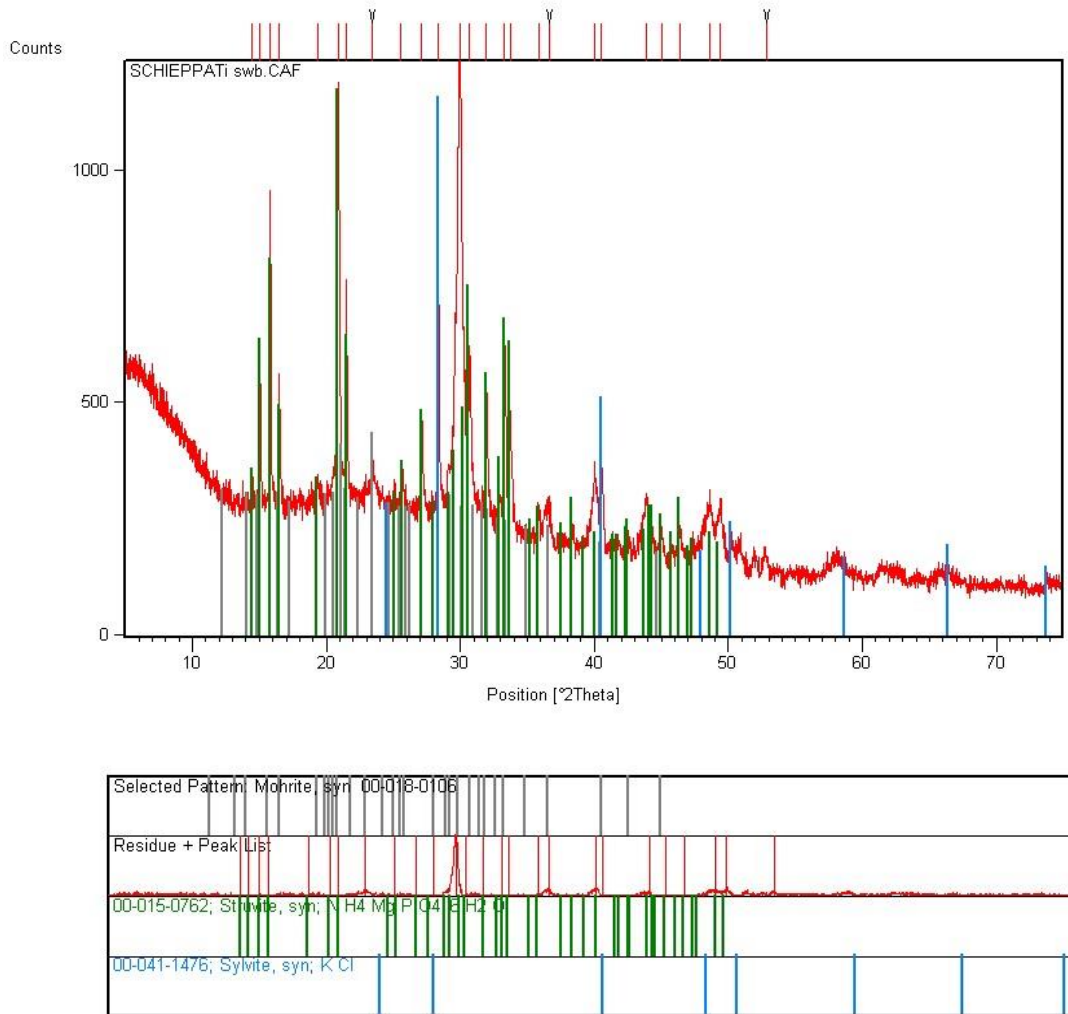


**Fig. 10** XRD diffractograms of struvite crystals recovered in SWB precipitation, showing the prevalence of the mineral in the samples analyzed.

## 4.2 Influent solution characterization

The different substrates used as influent solution in the crystallizer were characterized as described in the Chapter 3 and the collected data are presented in Table 6-8.

**Tab. 6** Chemical characterization of the swine manure liquid fraction (influent solution in Test 1-5)

Samples	DM <sup>a</sup> (g kg <sup>-1</sup> FM)	DM breakdown (%DM)	P <sub>tot</sub> <sup>b</sup> (g kg <sup>-1</sup> DM)	P <sub>tot</sub> breakdown (%DM)	TKN <sup>c</sup> (g kg <sup>-1</sup> DM)	TKN breakdown (%DM)	TOC <sup>d</sup> (g kg <sup>-1</sup> DM)
D	4.6 ± 1.2	100	28.3 ± 2.2	100	126 ± 0.7	100	2.4 ± 0.5
SF	185 ± 2.2	17.1	13 ± 2.4	9.7	32.6 ± 0.4	5.9	10.7 ± 1.5
LF	4.4 ± 0.3	82.9	25 ± 0.5	90.3	104 ± 0.4	94.1	2.7 ± 0.4

FR	97 ± 0.3	12.9	14.4 ± 1.7	8.9	58.8 ± 0.5	6.8	4.6 ± 0.6
F	33 ± 0.4	70	24.2 ± 1.8	81.4	139 ± 0.4	88.2	1.6 ± 0.7

Tab. 7 Chemical characterization of the cattle manure liquid fraction (influent solution in Test 6)

Samples	DM (g kg <sup>-1</sup> FM)	DM breakdown (%DM)	P <sub>tot</sub> (g kg <sup>-1</sup> DM)	P <sub>tot</sub> breakdown (%DM)	TKN (g kg <sup>-1</sup> DM)	TKN breakdown (%DM)	TOC (g kg <sup>-1</sup> DM)
D	51 ± 1.2	100	13.1 ± 1.2	100	72 ± 0.8	100	3.3 ± 0.3
SF	252 ± 2.5	25.8	11.9 ± 0.4	76.2	21.2 ± 0.4	91.8	11.2 ± 1.3
LF	46 ± 1.8	74.2	11 ± 1.3	25.8	78 ± 2.1	8.2	2.4 ± 0.5

Tab. 8 Chemical characterization of the OFMSW digestate (influent solution in Test 7)

Saples	DM (g kg <sup>-1</sup> FM)	DM breakdown (%DM)	P <sub>tot</sub> (g kg <sup>-1</sup> DM)	P <sub>tot</sub> breakdown (%DM)	TKN (g kg <sup>-1</sup> DM)	TKN breakdown (%DM)	TOC (g kg <sup>-1</sup> DM)
D	51 ± 1.3	100	26 ± 1.7	100	113 ± 8.3	100	5 ± 0.2
FR	123 ± 1.5	15.4	11.2 ± 0.9	17.4	47.2 ± 5.7	6.4	11.8 ± 1.6
F	45 ± 2.1	84.6	10.9 ± 0.7	82.6	127 ± 7.4	93.6	3.6 ± 0.6

D: Digestate; SF: Solid Fraction; LF: Liquid Fraction; FR: Filtration Residue; F: Filtrate

<sup>a</sup>DM: Dry Matter;

<sup>b</sup>P<sub>tot</sub>: total phosphorus

<sup>c</sup>TKN: Total Kjeldhal Nitrogen;

<sup>d</sup>TOC: Total Organic Carbon.

### 4.3 Swine manure test performances

#### 4.3.1 Crystallizer precipitation tests

In all the tests, P was the limiting compound for struvite formation, and the steady-state in P recovery was achieved within 5-10 days (start-up period). The results are presented in Tab. 9, showing the P-recovery efficiencies achieved at stable conditions for each test, the Mg<sup>2+</sup>/PO<sub>4</sub><sup>3-</sup> molar ratio, the TS percentage and the supersaturation value.



Tab. 9 Crystallizer phosphorus removal efficiency for each test

Test	Removal efficiency (%)	Mg <sup>2+</sup> /PO <sub>4</sub> <sup>3-</sup> ratio	TS (%)	Supersaturation (S <sub>c</sub> )
1	57.9 ± 6.2	1.8:1	3.3	1.6
2	84.2 ± 1.9	2:1	3.3	2.4
3	71.7 ± 6.6	3:1	3.3	1.7
4	76 ± 5.1	2:1	4.5	1.5
5	60.5 ± 5.8	3:1	4.5	1.4

In the Test 1, the phosphorus recovery efficiency reached in the reactor was 57.9 ± 6.2% phosphorus crystallization percentage, obtained using a Mg<sup>2+</sup>/PO<sub>4</sub><sup>3-</sup> molar ratio of 1.8:1 and a TS content of 3.5±0.2%, while the nitrogen recovery efficiency was 46 ± 4.2 %.

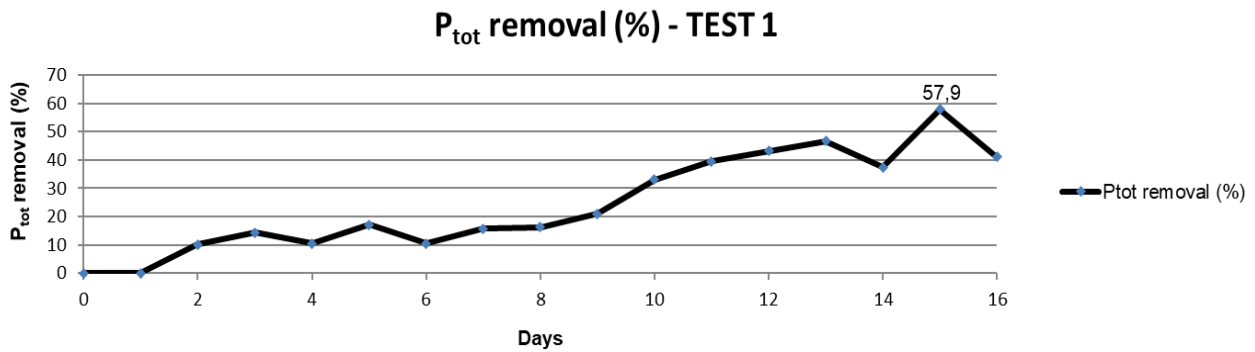


Fig. 10 Phosphorus removal (%) trend in Test 1

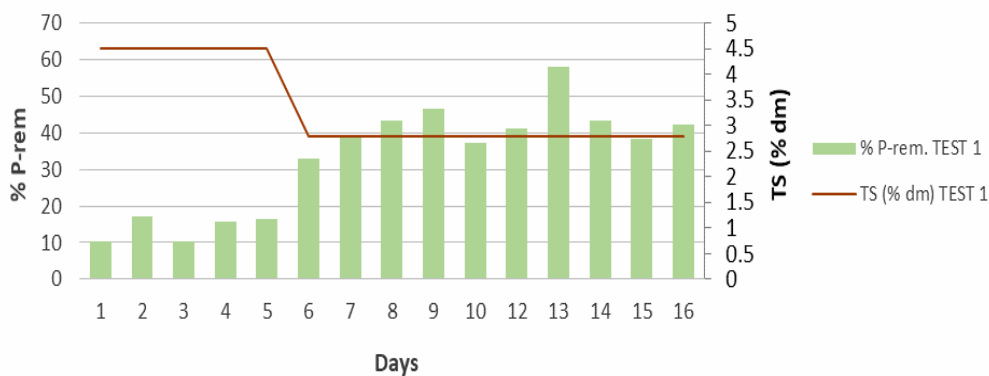
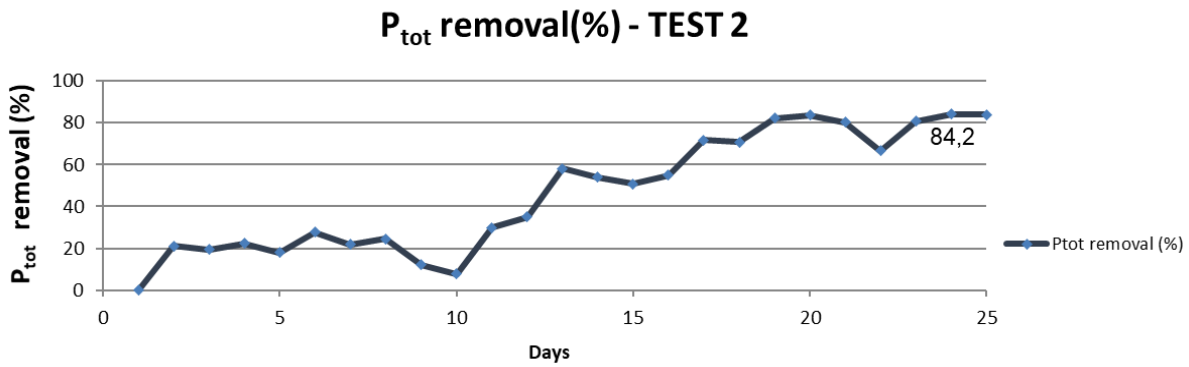
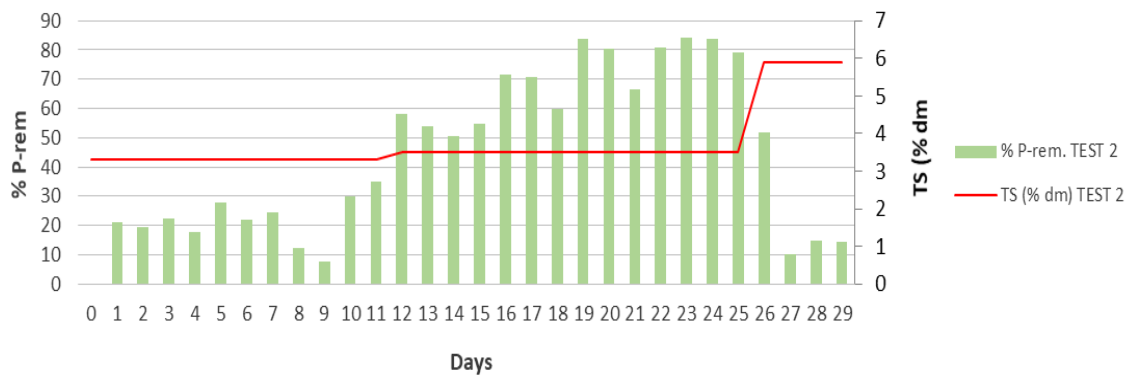


Fig. 11 Comparison between phosphorus removal and TS (%) concentration in Test 1

The following Test 2 was conducted with a  $Mg^{2+}/PO_4^{3-}$  molar ratio of 2:1, maintaining a TS content of  $3.5 \pm 0.2\%$ . The resulting recovery efficiency was higher than Test 1, removing the  $84.2 \pm 1.9\%$  of phosphorus and the  $52 \pm 3.2\%$  of nitrogen.



**Fig. 12** Phosphorus removal (%) trend in Test 2



**Fig. 13** Comparison between phosphorus removal and TS (%) concentration in Test 2

In Test 3 the  $Mg^{2+}/PO_4^{3-}$  molar ratio was changed in 3:1 (TS  $3.5 \pm 0.2\%$ ), obtaining the  $71.7 \pm 6.6\%$  of P removal and the  $31 \pm 4.7\%$  of N removal. Since these results it emerged that the best  $Mg^{2+}/PO_4^{3-}$  molar ratio were 2:1, 3:1 for working in the controlled environment of the reactor using swine manure liquid fraction with TS 3.3 %.

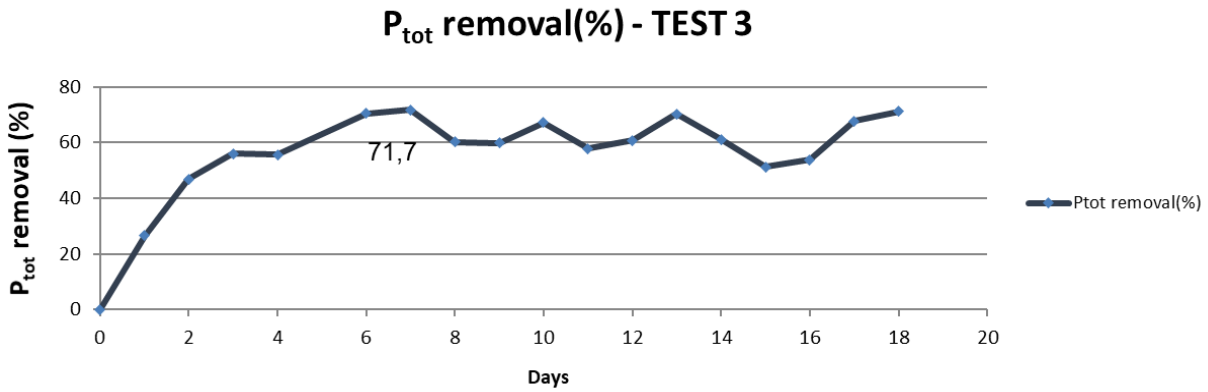


**Fig.14** Phosphorus removal (%) trend in Test 3

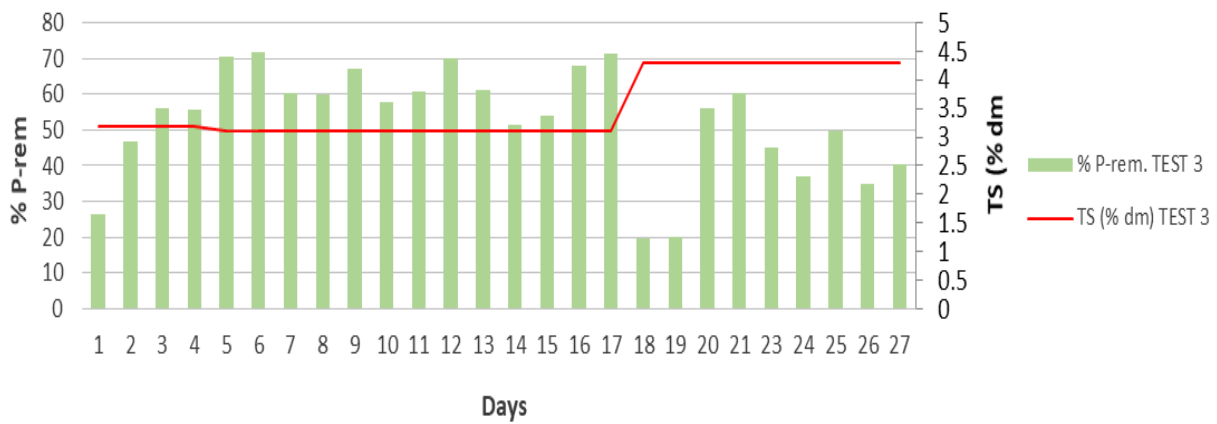


**Fig. 15** Comparison between phosphorus removal and TS (%) concentration in Test 3

The effects of increasing the TS content percentages to 4.5 were observed in Test 4 and 5, simulating the input of raw material (without any filtration or dilution) in the crystallizing system. Once fixed the best working condition of the previous Test 1-3, the influent solution with a  $Mg^{2+}/PO_4^{3-}$  molar ratio of 2:1 and TS 4.5% allowed to reach an efficiency of  $76 \pm 5.1\%$  of phosphorus removal and a  $38.9 \pm 2.1\%$  of nitrogen removal in trial n°4.

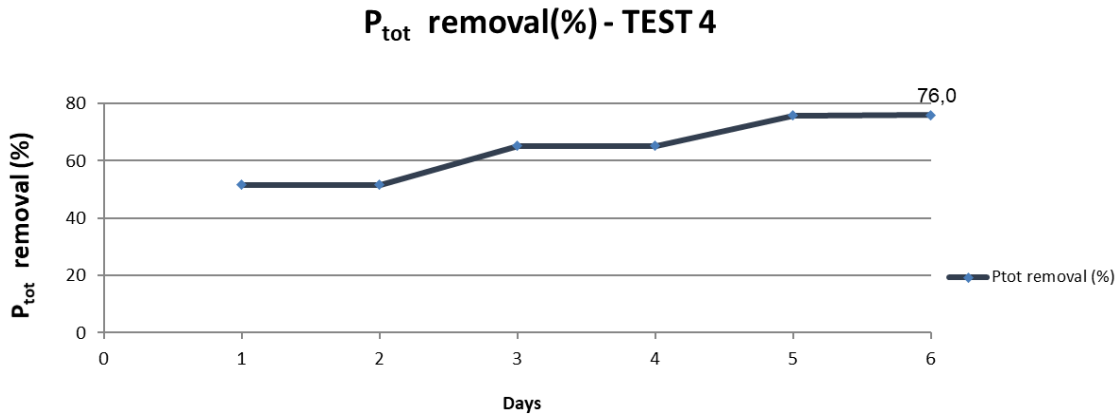


**Fig. 16** Phosphorus removal (%) trend in Test 4

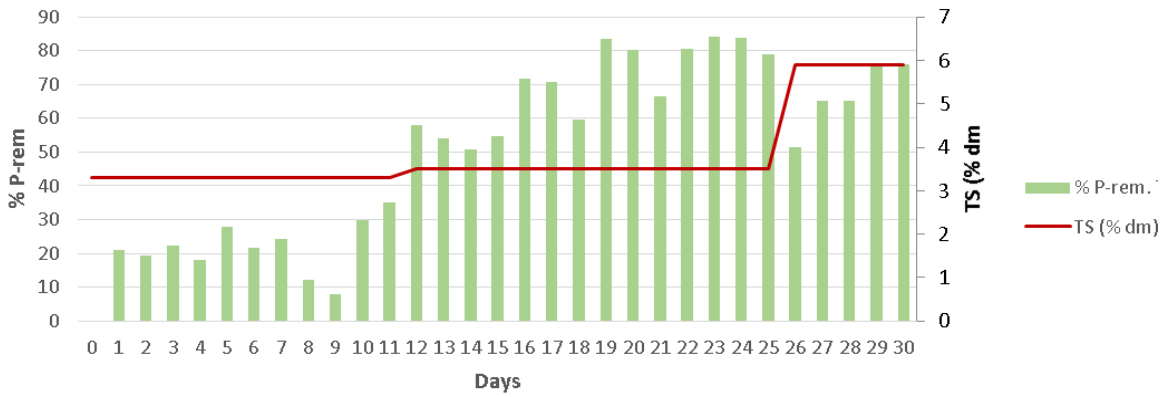


**Fig. 17** Comparison between phosphorus removal and TS (%) concentration in Test 4

In Test 5 the  $Mg^{2+}/PO_4^{3-}$  molar ratio was 3:1 and the respective phosphorus and nitrogen removal efficiencies were  $60.5 \pm 1.8 \%$  and  $33 \pm 3.6\%$ . In these two last tests the efficiency removal was lower than the precedent test, since the high amounts of suspended solids (TS >4%) and organic matter may limit the amount of struvite crystallized (Havukainen et. al, 2016).

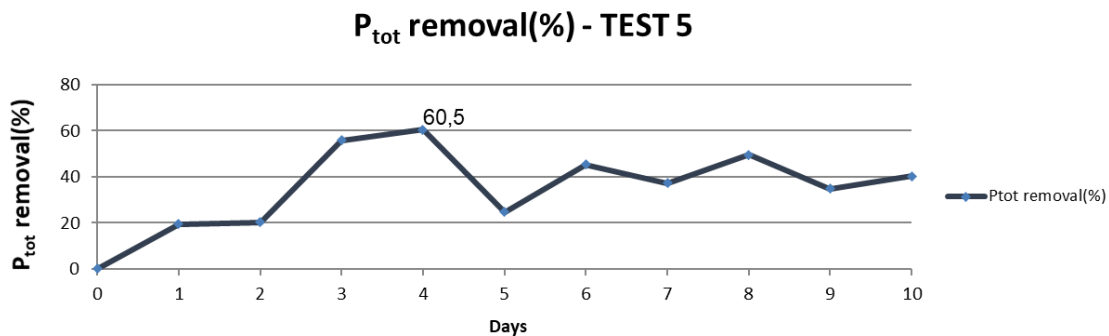


**Fig. 18** Phosphorus removal (%) trend in Test 5

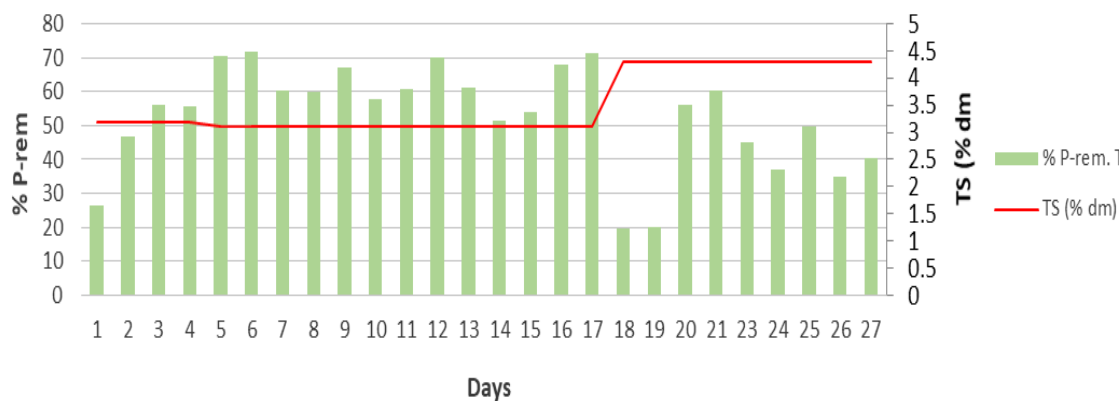


**Fig. 19** Comparison between phosphorus removal and TS (%) concentration in Test 5

Thus, the best crystallizer efficiency performances were reached in Test 2 and Test 4 (Tab. 10), respectively representative of low and high TS content and with an influent solution characterized by a  $Mg^{2+}/PO_4^{3-}$  molar ratio of 2:1. Considering the high phosphorus removal achieved in Test 2 and 4, these parameters were fixed in the following part of the study, in which was changed the type of the substrate.

Tab. 10 Chemical characterization of the output flow of Test 2 and 4

Sample	DM (g kg <sup>-1</sup> FM)	P <sub>tot</sub> (g kg <sup>-1</sup> DM)	TKN (g kg <sup>-1</sup> DM)	TOC (g kg <sup>-1</sup> DM)	Mg (g kg <sup>-1</sup> DM)	Ca (g kg <sup>-1</sup> DM)	K (g kg <sup>-1</sup> DM)	Fe (g kg <sup>-1</sup> DM)
OUT 2	38.6 ± 0.8	46 ± 4.7	92.3 ± 4.1	42.1 ± 1.3	15.2 ± 2.2	41.0 ± 0.8	47 ± 0.9	3.4 ± 0.2
OUT 4	71 ± 0.9	55.2 ± 3	62 ± 2.7	29.6 ± 2.1	36.2 ± 4.2	54.1 ± 1.7	21 ± 3.4	4.7 ± 0.9

#### *4.3.2 Repartition of dry matter, phosphorus and nitrogen*

Data reported in Table 1 show the repartition of the dry matter in the solid and liquid fractions determined by using Eq. 4. As illustrated in Fig.6 the 17.1% (as average) of the total DM of digestate went to the SF and the 82.9% (as average) remained in the LF. In Test 2 the filtration of the LF determine another separation of the dry matter: the 9.5% (as average) of the LF dry matter went in the filtration residue (FR), while the 73.4% remained in the filtered liquid (F).

Based on the DM breakdown it was then estimated the repartition of total P and TKN, from the initial digestate to the final output of the crystallizer (Fig. 20). The 70 % of total P and the 46 % of TKN of the digestate runs out of the collector during the maximum efficiency interval of Test 2 (crystallizer internal removal efficiency:  $84.2 \pm 1.9\%$ ).

In Test 4 the 75.4% (as average) of the digestate total DM went in the raw material lightly filtered (F), while the remaining 7.5% went in the FR (Fig. 21). Considering that in the Test 4 the highest crystallizer internal efficiency was  $76 \pm 5.1\%$ , it was then estimated that the 65 % of total P and the 34% of TKN of the digestate runs out of the collector.

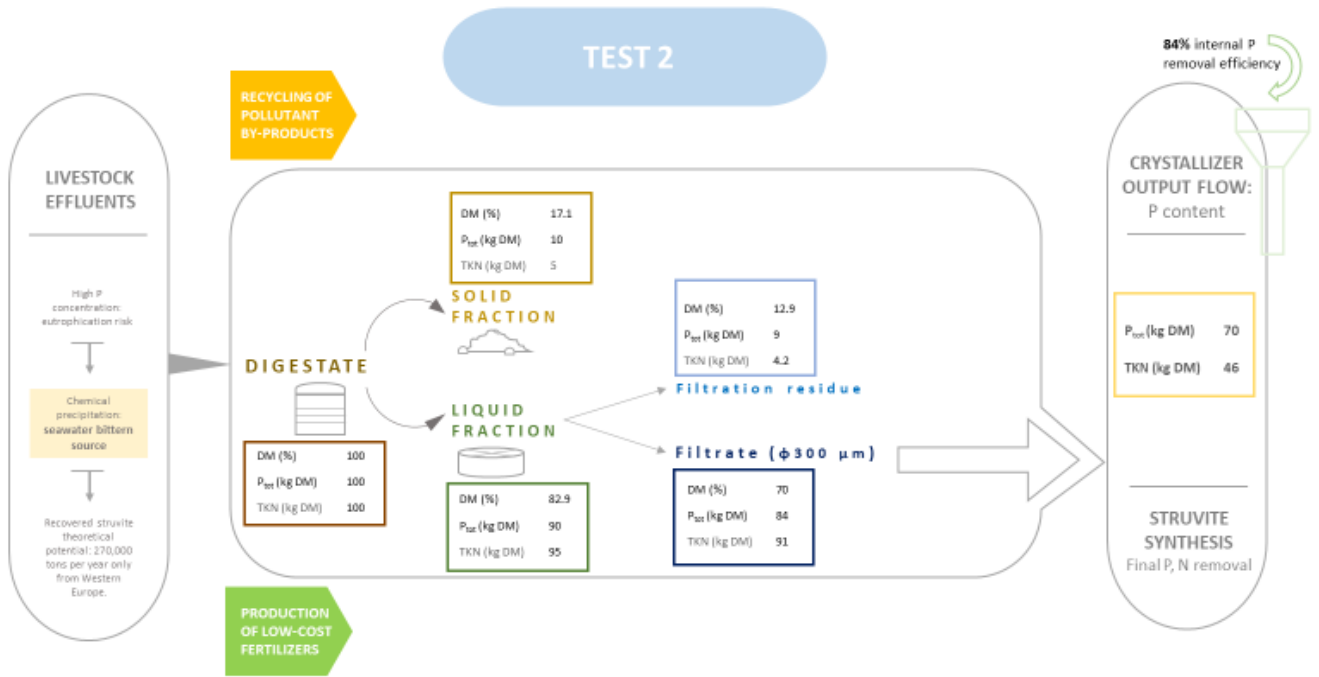


**Fig. 20** Mass balance of Test 2

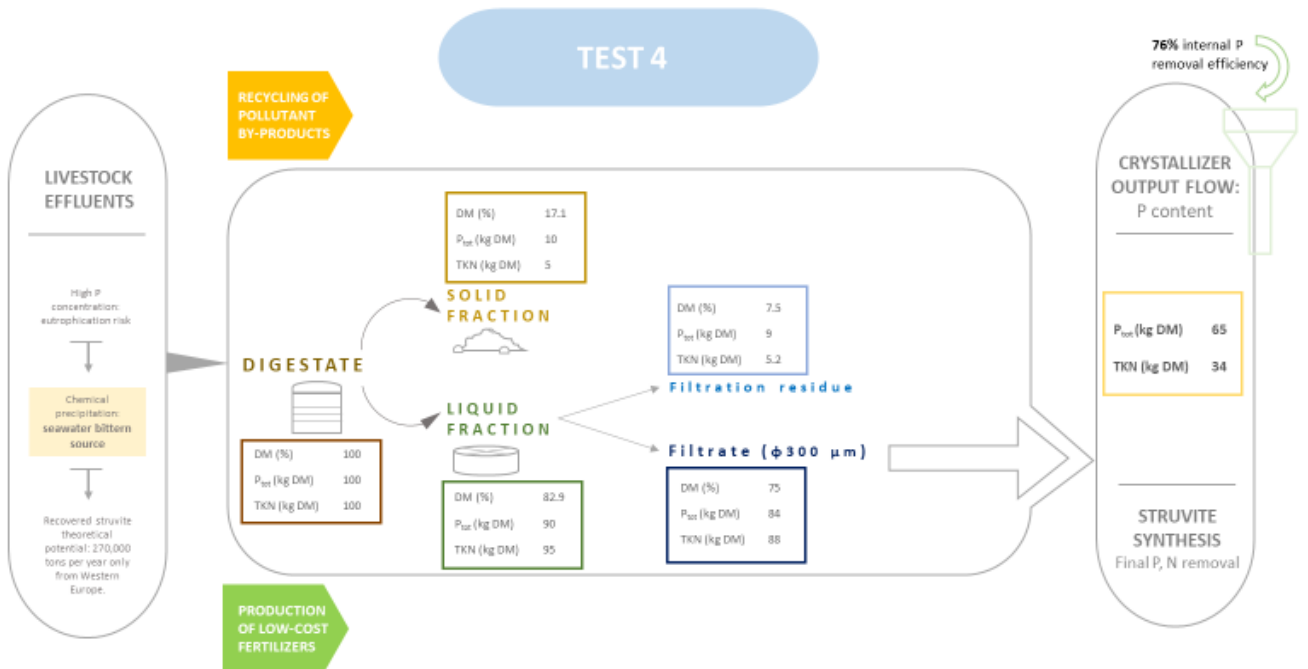


**Fig. 21** Mass balance of Test 4

#### 4.3.3 Optical microscopy analyses on the recovered product

Microscopic analyses on both the effluent and collector flows revealed many differences in the samples, which allowed to study the path of organic and inorganic particles and crystals formation. Effluent flows were characterized (in all the Test 1-5) by a raw distribution of organic and inorganic materials, no presence of crystalline structures and a strong aggregation between particles (Fig. 22). Collector flows showed presence of many crystals with a diameter between 100-300  $\mu\text{m}$ , characterized by different crystalline structures, in the majority prismatic and cubic. In some samples were identified dendritic structures with bigger dimension (500  $\mu\text{m}$ ), grown on a nucleus of organic matter and spread homogeneously in the sample. These structures are possibly indicative of the formation of a small amount of larger crystals rather than a greater quantity of smaller ones, a process depending most on the pH of the inner reactor environment (Prywer et al., 2012; Rouff, 2013; Stolzenburg et al., 2014). In fact, dendritic crystals appear when the reactor system undergoes rapid pH changes and there are large amounts of Mg in the solution (Prywer et al., 2012; Rouff, 2013; Stolzenburg et al., 2014)

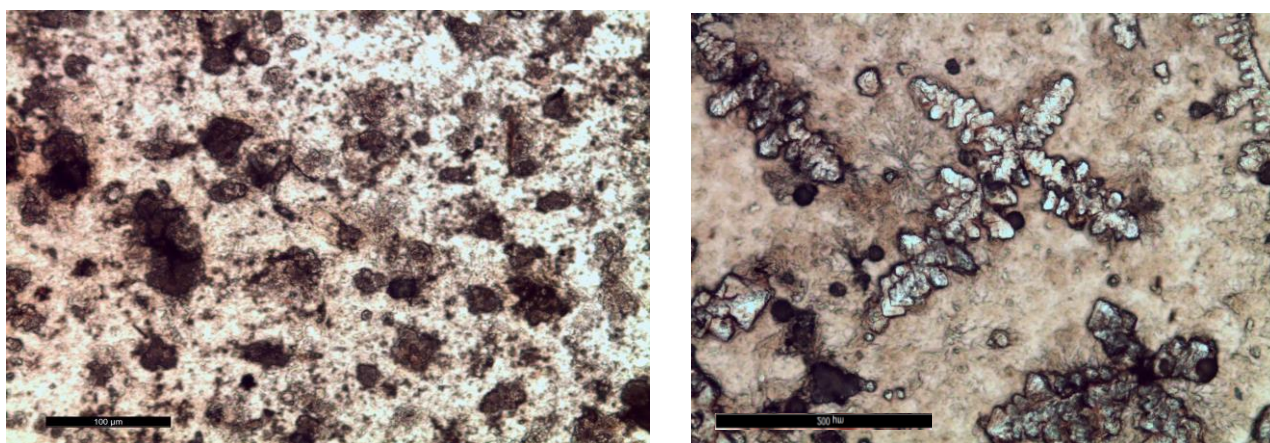


**Fig. 22** Optical microscopy analyses of effluent (left) and collector (right) samples with dendritic structures



#### 4.3.4 X-ray diffraction (XRD) analyses

The recovered samples of Test 2 and 4 were analyzed by X-ray diffraction (XRD). This method was performed to quantitatively determine the crystal phases and amorphous content of struvite samples. XRD analyses exhibited several peaks indicative of the presence of struvite in the collector samples. In the specific the samples corresponding to the highest P removal showed the exclusive presence of struvite crystals (Fig. 23). These results indicated that the quality of the struvite recovered was not influenced also in presence of high concentration of TS (4.5 %), as already observed by Tarragò et al. (2018).

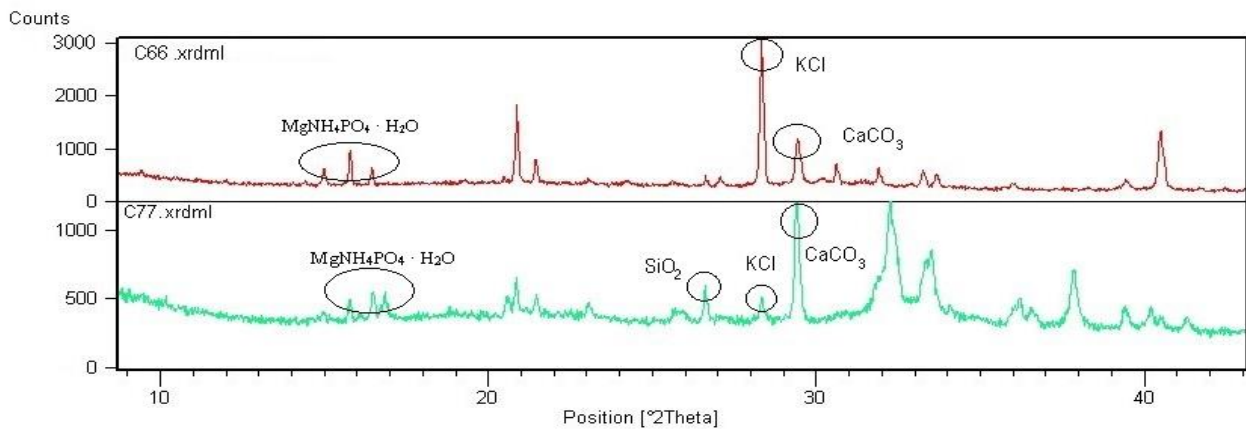


**Fig. 23** X-ray diffractogram of the output flow of Test 2 (red) and Test 4 (green)

#### 4.3.5 Agronomic performances

Agronomic tests were performed to assess the fertilizing properties of the final product collected in all the tests in comparison with the performances of common mineral phosphate fertilizers and poultry manure. The results show a significant difference between the samples grown with no added fertilizers (control samples) and the other cultivated with struvite, poultry manure and common mineral fertilizer. In the specific, among these the best performances in terms of nutrient adsorbed, height and plant wealth were reached using the two organic fertilizers, poultry manure and struvite,

which gave similar results (Fig. 24). The control specimens show lack of nutrients (nitrogen content), low heights and less vivid colors in the leaves, in comparison with the fertilized plants. In particular, samples fertilized with struvite show higher nitrogen and chlorophyll content (Tab. 4). This is presumably due to the organic fraction included in the struvite collected during the tests in the reactor, which allows higher efficiencies in cultivation, as expected (Feifei et al., 2011).



**Fig. 24** Pot-trials at different steps of the experimentation

Tab. 11 Agronomic performances

Samples	Biomass (g)	TKN (g kg <sup>-1</sup> )	P <sub>tot</sub> (g kg <sup>-1</sup> )	Chlorophyll A (g kg <sup>-1</sup> )	Chlorophyll B (g kg <sup>-1</sup> )
Ø	22.9 ± 1.14	19.8 ± 0.7	1.1 ± 0.1	817 ± 66	286 ± 29
M	42.1 ± 5.3	56.6 ± 0.9	5.6 ± 0.4	1520 ± 12	478 ± 1
P	60.9 ± 5.6	51.3 ± 7.4	5.7 ± 0.2	1498 ± 189	497 ± 57
S	50.9 ± 16.9	62.3 ± 3.0	5.9 ± 0.1	1565 ± 91	522 ± 39

Ø: control samples, no fertilizers added; M: samples with mineral fertilizer added; P: samples fertilized with poultry manure; S: samples fertilized with the collected struvite.

#### 4.3.6 Phosphorus speciation

Results of phosphorus fractionation analyses show a higher P content in the crystallizer's struvite than in poultry manure samples. This is indicative of the higher fertilizing power of struvite in

comparison with common mineral and organic fertilizers, due both to its elevated P content and to P availability, which is 3.3 times greater than in poultry manure.

Data collected show a concentration of 84% of available P in poultry manure and 71% in struvite. In particular, poultry manure contains more phosphorus bounded to aluminum/iron and organic P (extracted by NaOH+EDTA) than struvite (29%), which is probably related to the high organic matter content in poultry manure.

Phosphorus quantifiable with HCl extraction (calcium phosphates) is higher in poultry manure (43%) than in struvite (37%). This is presumably due to the elevated Mg content in the crystallizer, determined by a steady input of the seawater bittern solution which caused a Mg-phosphate precipitation rather than a Ca-phosphate (less soluble).

#### 4.4 Cattle manure test performances

##### 4.4.1 Crystallizer precipitation tests

In Test 6, as for other tests, the steady-state in P recovery was achieved within 5-7 days (start-up period). The results are presented in Tab. 12 showing the P-recovery efficiencies achieved at stable conditions for each test, the  $Mg^{2+}/PO_4^{3-}$  molar ratio, the TS percentage and the supersaturation value.

Tab. 12 Crystallizer phosphorus removal efficiency for Test 6

Test	Removal efficiency (%)	$Mg^{2+}/PO_4^{3-}$ ratio	TS (%)	Supersaturation ( $S_c$ )
1	$59.7 \pm 3.2$	2:1	$4.5 \pm 0.3$	2.6

In this trial the phosphorus recovery efficiency reached in the reactor was  $59.7 \pm 3.2\%$ , obtained using a  $Mg^{2+}/PO_4^{3-}$  molar ratio of 2:1 and a TS content of  $4.5 \pm 0.3\%$ , while the nitrogen recovery efficiency was  $31 \pm 3.2\%$  (Fig. 25-26). Comparing these results with Test 4 outcomes, considered

as starting point for the trial with high solids content (TS > 4%), it was observed that the efficiencies in phosphorus and nitrogen removal for the Test 6 were lower comparing with results previously reached Test 4. Nevertheless, cattle influent solution has a higher OM content (Tab. 7) comparing to swine substrate, which may affect struvite precipitation (Stolzenburg et al., 2014). Stolzenburg et al. (2014) demonstrated that organic matter reduces the kinetics of struvite crystallization due to the viscosity generated by the repulsive force of the colloids.

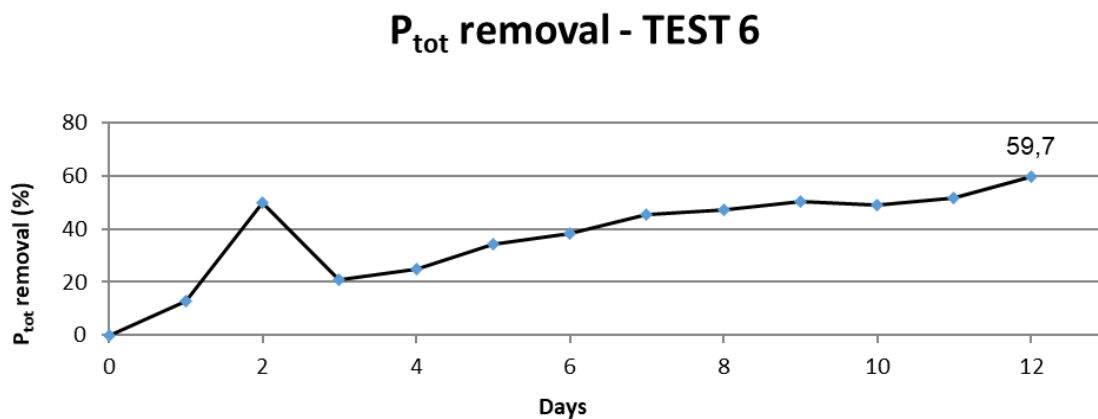


**Fig. 25** Phosphorus removal (%) trend in Test 6

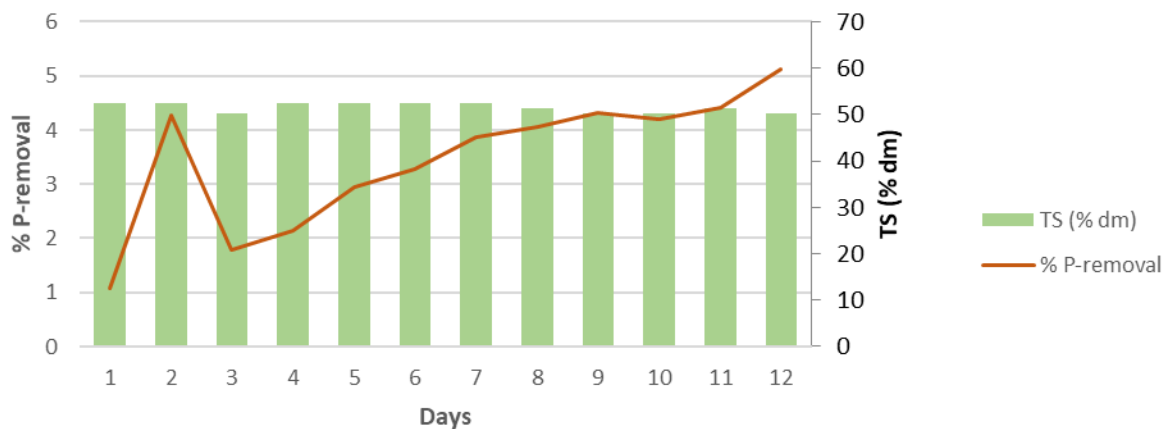


**Fig. 26** Comparison between phosphorus removal and TS (%) concentration in Test 6

#### 4.4.2 Repartition of dry matter, phosphorus and nitrogen

Data reported in Table 7 show the repartition of the dry matter in the solid and liquid fractions determined by using Eq. 4. As illustrated in Fig. 27 the 25.2% (as average) of the total DM of digestate went to the SF and the 74.8% (as average) remained in the LF. Comparing these results with data from previous tests, it could be noticed that the DM concentration in LF is here sensibly lower. This is presumably related to many factors depending on the manure type, as the high OM rate, particles size, the presence of colloids, which may interfere with the repartition of dry matter (Burton et al., 2003; Møller et al., 2007).

Based on the DM breakdown it was then estimated the repartition of total P and TKN, from the initial digestate to the final output of the crystallizer (Fig. 27). The 44% of total P and the 27% of TKN of the digestate runs out of the collector during the maximum efficiency interval of Test 6 (crystallizer internal removal efficiency for phosphorus:  $59.7 \pm 3.2\%$ ).

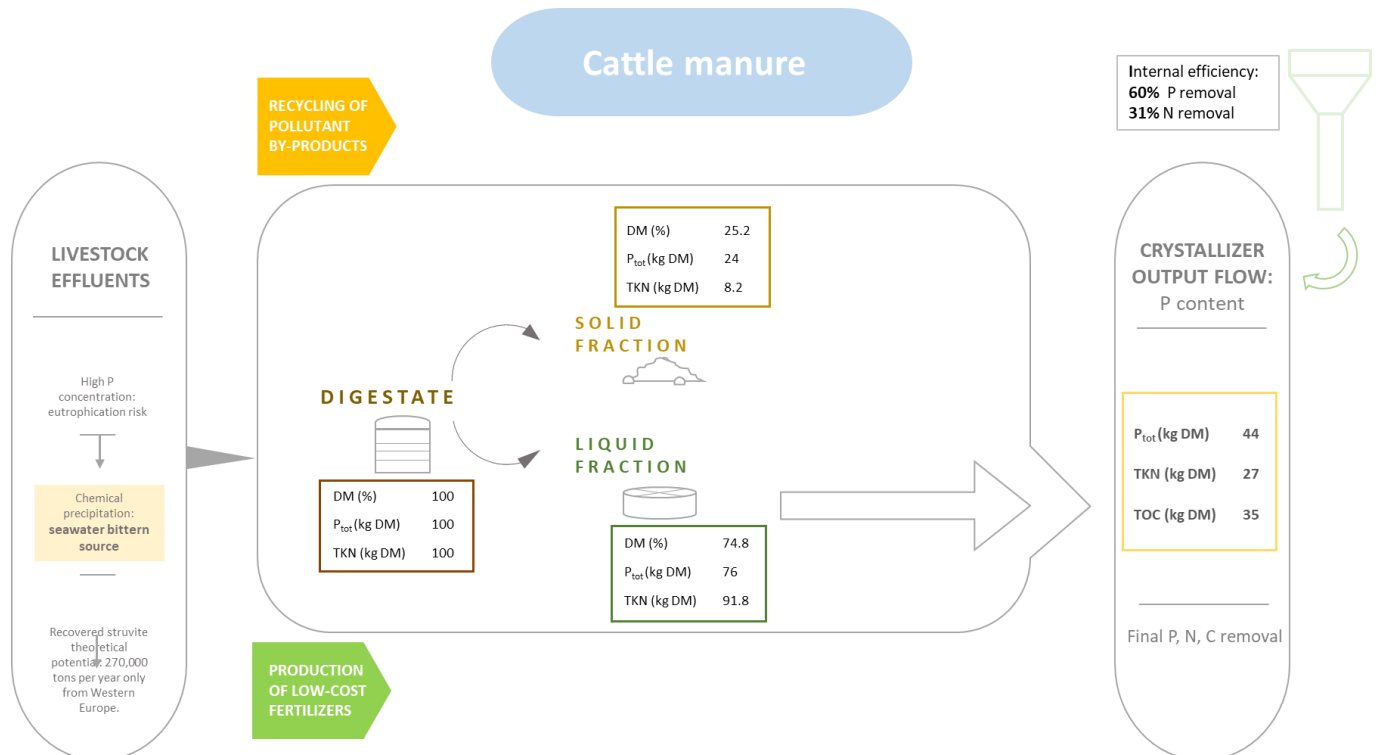


**Fig. 27** Schematization of mass balance in Test 6

#### 4.4.3 Optical analyses on the recovered product

Microscopic analyses on both the effluent and collector flows revealed many differences in the samples, which allowed to study the path of organic and inorganic particles and crystals formation. Effluent flows were characterized by a raw distribution of organic and inorganic materials, no presence of crystalline structures and a strong aggregation between particles (Fig. 28). Collector flows showed presence of crystals with a diameter between 30-50  $\mu\text{m}$ , characterized by different crystalline structures, in the majority prismatic and cubic (Fig. 26). Optical analyses highlight a minor incidence of crystals in comparison with previous tests.

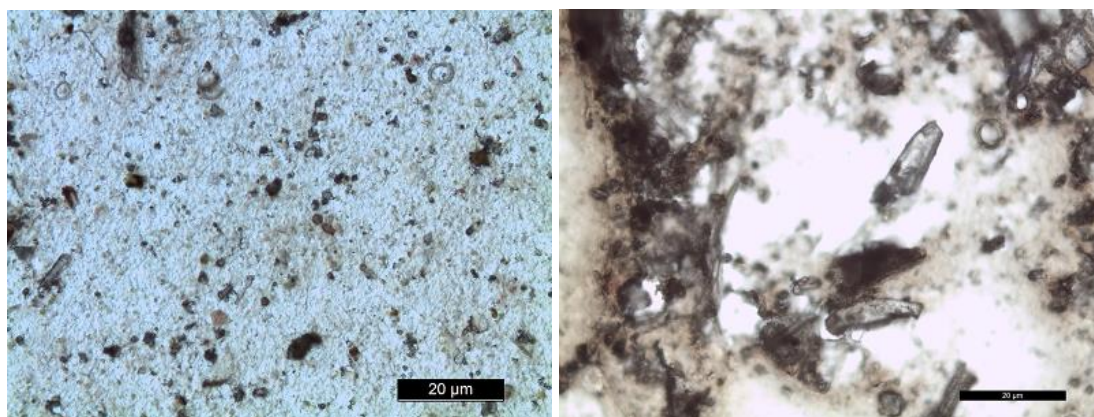


**Fig. 28** Optical microscopy analyses of effluent (left) and collector (right) samples

#### 4.4.4 X-ray diffraction (XRD) analyses

Samples recovered from the crystallizer output were characterized by XRD analysis. Crystals previously observed through optical microscopy were identified as sylvite (KCl) and magnesium-rich calcite ((Ca,Mg)CO<sub>3</sub>), while the precipitation of phosphorus occurred in the amorphous form. As previously observed in other studies (Rittmann et al., 2011; Shih and Yan, 2016; Suci Perwitasari et al., 2016) high Ca<sup>2+</sup> rates inhibit the struvite precipitation, leading to the formation of

many crystals rather than crystalline struvite. Nevertheless, the amount of P removed is sensibly high and the precipitation in the amorphous form is visible in the XRD diffractogram as a well-developed curve in correspondence of phosphates.

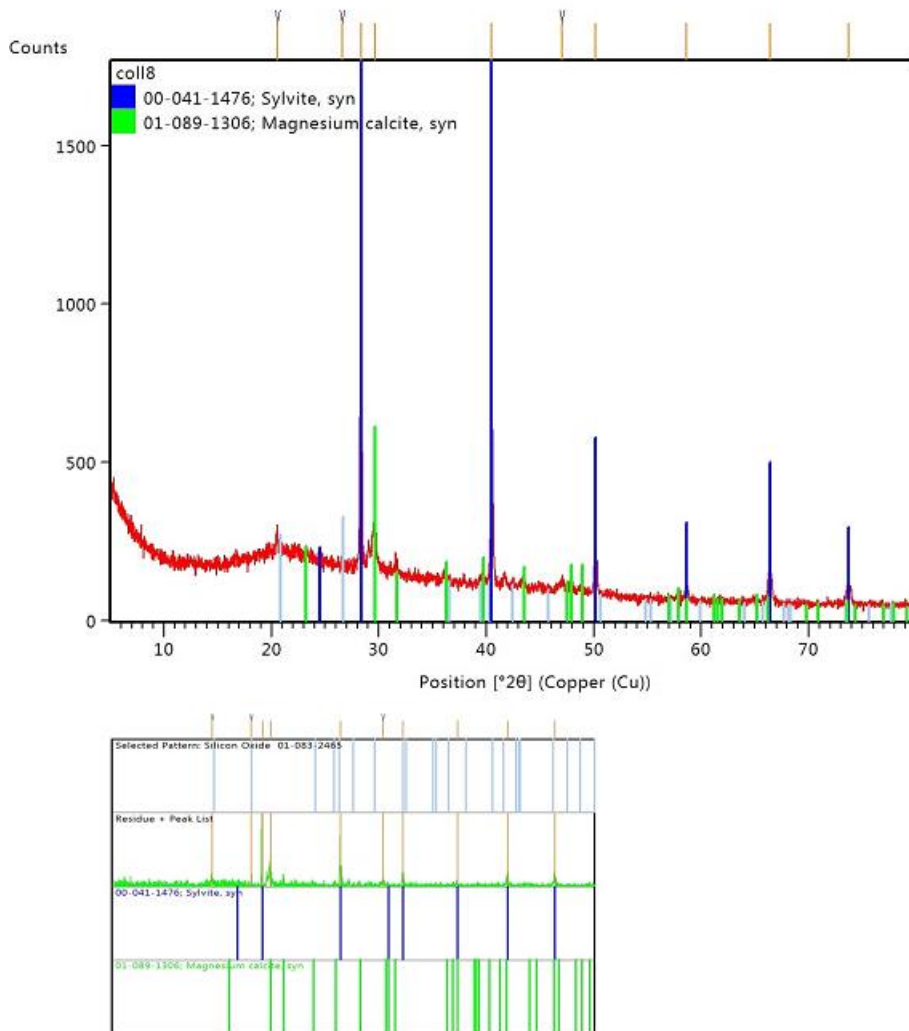


**Fig. 29** XRD diffractogram of the output flow recovered (Test 6)

#### 4.4.5 Agronomic performances

Agronomic tests were performed to assess the fertilizing properties of the final product collected in all the tests in comparison with the performances of common mineral phosphate fertilizers and poultry manure. The results show a significant difference between the samples grown with no added



fertilizers (control samples) and the other cultivated with struvite, poultry manure and common mineral fertilizer. In the specific, in contrast with previous results reached with swine struvite, the product recovered in Test 6 gave inconclusive results (Fig. 30). The struvite specimens show lack of nutrients (nitrogen content) and low heights in comparison with control, M and P samples. Further analyses need to be performed to assess the causes of the growth failure in plants.

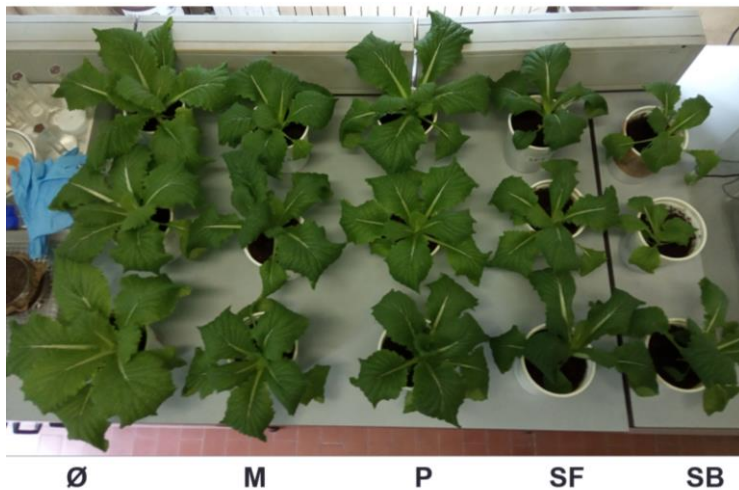


**Fig. 24** Pot-trials comparison. From left to right: control samples, mineral fertilizer (M), poultry manure (P), OFMSW precipitated (SF) and cattle fertilizer product (SB).



## 4.5 OFMSW manure test performances

### 4.5.1 Crystallizer precipitation tests

In Test 7, as for other tests, the steady-state in P recovery was achieved within 5-7 days (start-up period). The results are presented in Tab. 13 showing the P-recovery efficiencies achieved at stable conditions for each test, the  $Mg^{2+}/PO_4^{3-}$  molar ratio, the TS percentage and the supersaturation value.

Tab. 13 Crystallizer phosphorus removal efficiency for Test 7

Test	Removal efficiency (%)	$Mg^{2+}/PO_4^{3-}$ ratio	TS (%)	Supersaturation ( $S_c$ )
1	$67 \pm 4.7$	2:1	$4.5 \pm 0.7$	1.09

In this trial the phosphorus recovery efficiency reached in the reactor was  $67 \pm 4.7\%$ , obtained using a  $Mg^{2+}/PO_4^{3-}$  molar ratio of 2:1 and a TS content of  $4.5 \pm 0.7\%$ , while the nitrogen recovery efficiency was  $30 \pm 7.2\%$ . Comparing these results with Test 4 outcomes, considered as starting point for the trial with high solids content ( $TS > 4\%$ ), it was observed that the efficiencies in phosphorus and nitrogen removal for the Test 7 were lower comparing with results previously reached Test 4 (Fig. 30-31). Nevertheless, OFMSW influent solution has a higher OM content (Tab. 7) comparing to swine substrate, which may affect struvite precipitation (Stolzenburg et al., 2014). Stolzenburg et al. (2014) demonstrated that organic matter reduces the kinetics of struvite crystallization due to the viscosity generated by the repulsive force of the colloids.

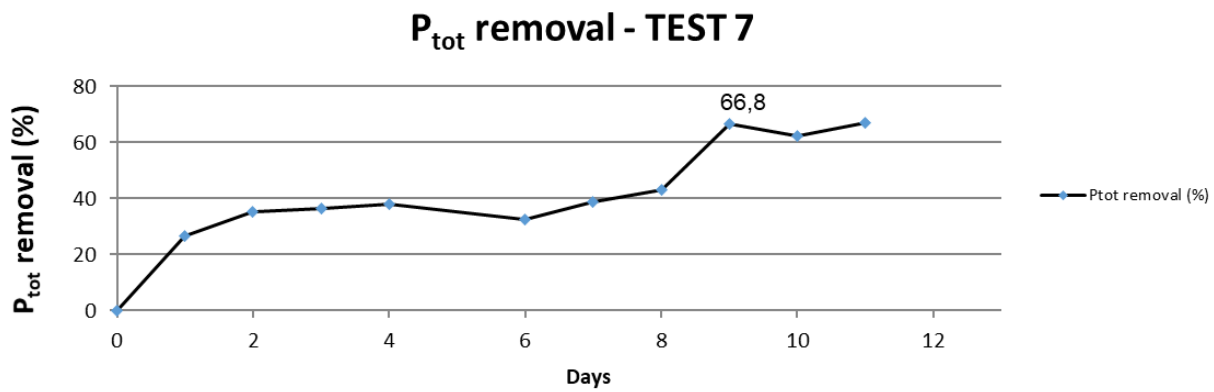


**Fig. 30** Phosphorus removal (%) trend in Test 7

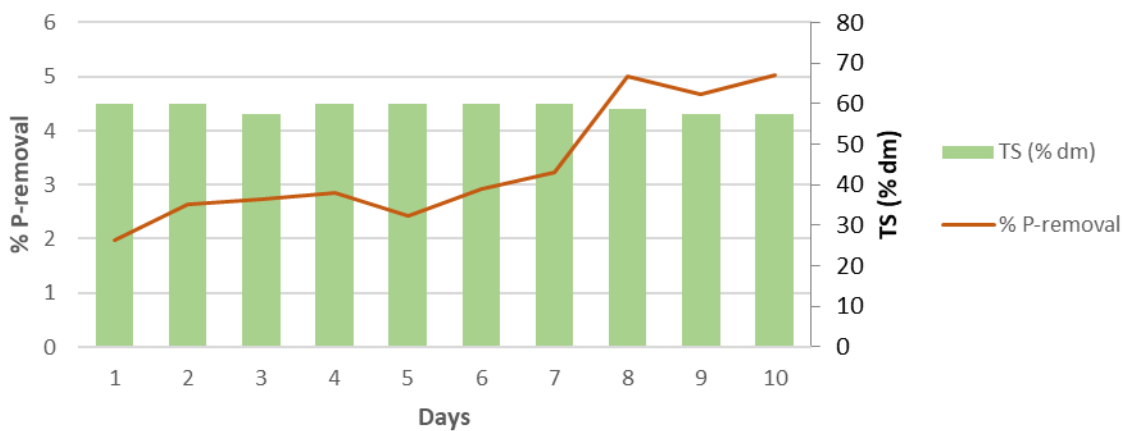


**Fig. 31** Comparison between phosphorus removal and TS (%) concentration in Test 7

#### 4.5.2 Repartition of dry matter, phosphorus and nitrogen

Data reported in Table 8 show the repartition of the dry matter in the solid and liquid fractions determined by using Eq. 4. As illustrated in Fig. 32 the 15.4% (as average) of the total DM of digestate went to the SF and the 84.6% (as average) remained in the LF. Comparing these results with data from Test 6, it could be noticed that the DM concentration in LF is here sensibly higher, similar to values observed in Test 1-5. This is presumably related to many factors depending on the manure type, as the high OM rate, particles size, the presence of colloids, which may interfere with the repartition of dry matter (Burton et al., 2003; Møller et al., 2007).

Based on the DM breakdown it was then estimated the repartition of total P and TKN, from the initial digestate to the final output of the crystallizer (Fig. 32). The 56 % of total P and the 28 % of TKN of the digestate runs out of the collector during the maximum efficiency interval of Test 6 (crystallizer internal removal efficiency for phosphorus:  $66.8 \pm 4.1 \%$ ).

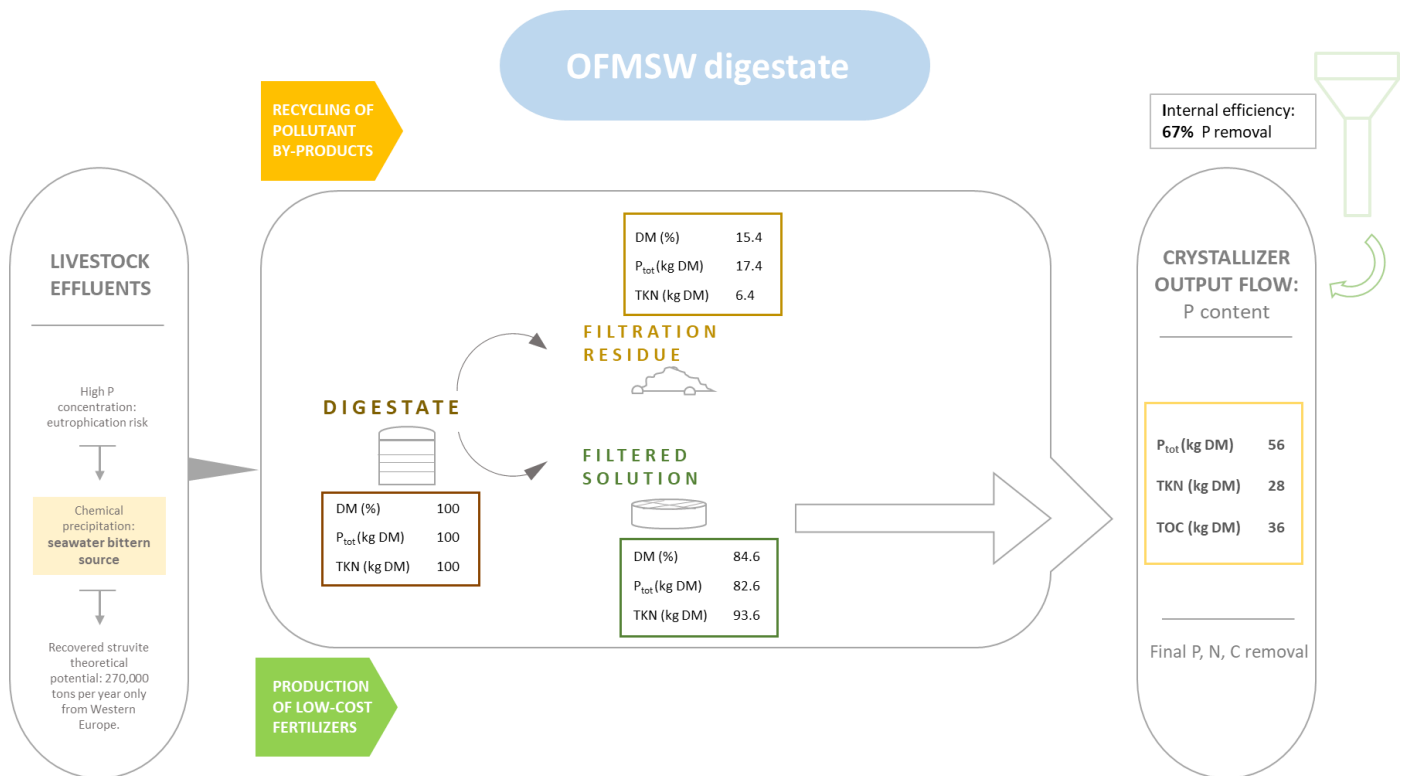


**Fig. 32** Schematization of mass balance in Test 7

#### 4.5.3 Optical analyses on the recovered product

Microscopic analyses on both the effluent and collector flows revealed many differences in the samples, which allowed to study the path of organic and inorganic particles and crystals formation. Effluent flows were characterized by a raw distribution of organic and inorganic materials, no presence of crystalline structures and a strong aggregation between particles (Fig. 33). Optical analyses highlight a minor incidence of crystals in comparison with Test 1-5.

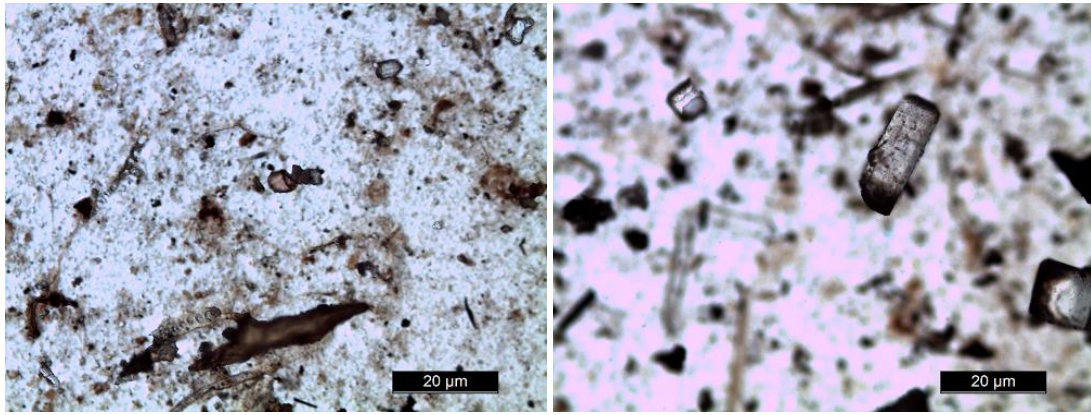


**Fig. 33** Optical microscopy analyses of effluent (left) and collector (right) samples

#### 4.5.4 X-ray diffraction (XRD) analyses

Samples recovered from the crystallizer output were characterized by XRD analysis. Crystals previously observed through optical microscopy were identified as sylvite (KCl), halite (NaCl) and aragonite ( $\text{CaCO}_3$ ), while the precipitation of phosphorus occurred in the amorphous form (Fig. 34). As indicated before, high  $\text{Ca}^{2+}$  rates inhibit the struvite precipitation, leading to the formation of many crystals rather than crystalline struvite (Rittmann et al., 2011; Suci Perwitasari et al., 2016; Yan and Shih, 2016). Nevertheless, the amount of P removed is sensibly high and the precipitation in the amorphous form is visible in the XRD diffractogram as a well-developed curve in correspondence of phosphates.

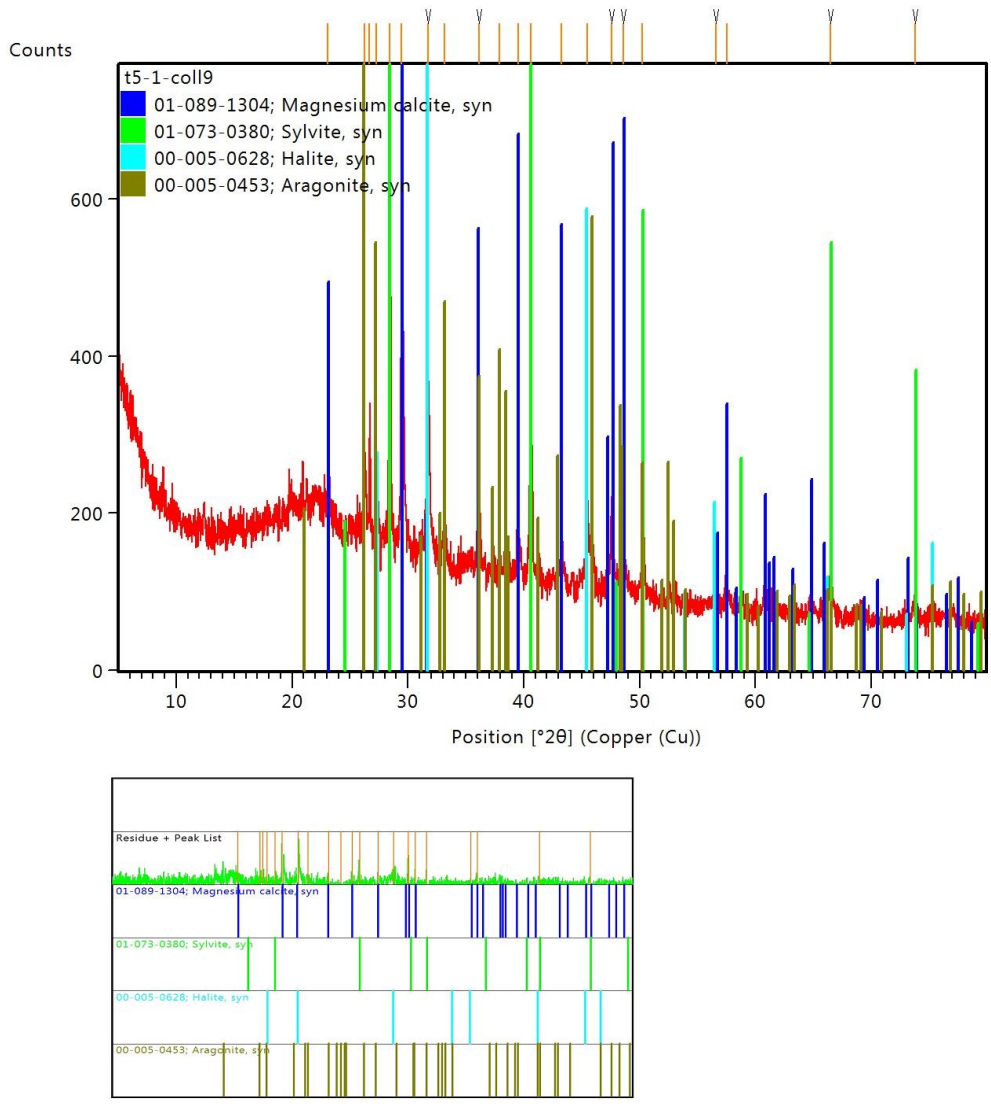


**Fig. 34** XRD diffractogram of the output flow recovered (Test 7)

#### 4.5.5 Agronomic performances

Agronomic tests were performed to assess the fertilizing properties of the final product collected in all the tests in comparison with the performances of common mineral phosphate fertilizers and poultry manure. The results show a significant difference between the samples grown with no added fertilizers (control samples) and the other cultivated with struvite, poultry manure and common mineral fertilizer. In the specific, in contrast with previous results reached with swine struvite, the product recovered in Test 6 gave inconclusive results (Fig. 35). The struvite specimens show lack of

nutrients (nitrogen content) and low heights in comparison with control, M and P samples. Further analyses need to be performed to assess the causes of the growth failure in plants.

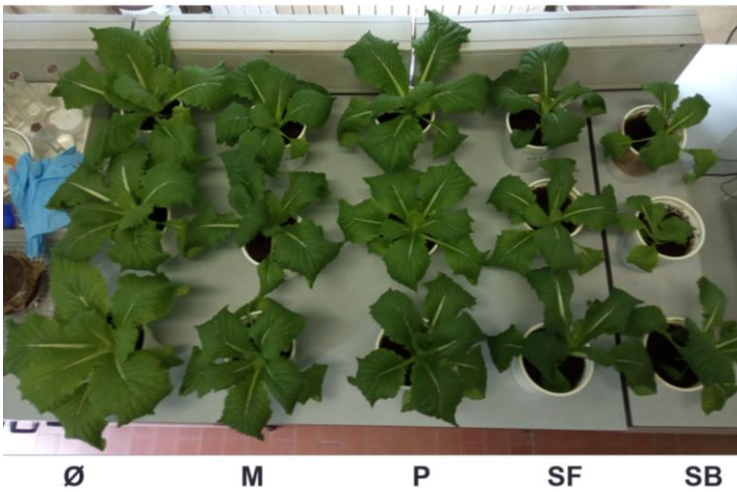


**Fig. 35** Pot-trials comparison. From left to right: control samples, mineral fertilizer (M), poultry manure (P), OFMSW precipitated (SF) and cattle fertilizer product (SB).

## 5. CONCLUSIONS

From the analysis performed in this study on P recovery from different substrates through struvite synthesis, some considerations are emerged.

Preliminary analysis showed that struvite crystallization is the best P removal system, above all if it is combined with the use of seawater bittern as a low-cost Mg source. Moreover, energetic and economic analysis revealed the value of the seawater bittern struvite as a competitive alternative to conventional phosphate fertilizers. The operative choice to maintain the  $Mg^{2+}/PO_4^-$  ratio at 2:1 it has been effective in all the tests performed, obtaining a P removal between 84% and 59% using different influent solutions. Phosphorus recovery by air-lift crystallizer technology has been already tested in wastewater treatment plants and data reported in this study showed the feasibility of this technology also in treating high total solids livestock manure (TS>4%), reaching over 70% of P removal.

Another main issue is the agronomic value of this recovered fertilizer. Test 1-5 gave important results, showing the best growth performances with the addition of the collected struvite. On the opposite, the plants growth failure in Test 6-7 open new perspectives, which need to be investigated, on the manure composition and on the possible interferences with plants health.

## References

- Angst, T.E., Sohi, S.P., 2013. Establishing release dynamics for plant nutrients from biochar. *GCB Bioenergy* 5, 221–226. <https://doi.org/10.1111/gcbb.12023>
- Ashley, K., Cordell, D., Mavinic, D., 2011. A brief history of phosphorus: From the philosopher's stone to nutrient recovery and reuse. *Chemosphere* 84, 737–746. <https://doi.org/10.1016/j.chemosphere.2011.03.001>
- Attour, A., Touati, M., Tlili, M., Ben Amor, M., Lopicque, F., Leclerc, J.-P., 2014. Influence of operating parameters on phosphate removal from water by electrocoagulation using aluminum electrodes. *Sep. Purif. Technol.* 123, 124–129. <https://doi.org/https://doi.org/10.1016/j.seppur.2013.12.030>
- Azuara, M., Kersten, S.R.A., Kootstra, A.M.J., 2013. Recycling phosphorus by fast pyrolysis of pig manure: Concentration and extraction of phosphorus combined with formation of value-added pyrolysis products. *Biomass and Bioenergy* 49, 171–180. <https://doi.org/https://doi.org/10.1016/j.biombioe.2012.12.010>
- Bedussi, F., Zaccheo, P., Crippa, L., 2015. Pattern of pore water nutrients in planted and non-planted soilless substrates as affected by the addition of biochars from wood gasification. *Biol. Fertil. Soils* 51.
- Bergmans, B., 2011. Struvite recovery from digested sludge at {WWTP} West.
- Bouamra, F., Drouiche, N., Ahmed, D.S., Lounici, H., 2012. Treatment of Water Loaded With Orthophosphate by Electrocoagulation. *Procedia Eng.* 33, 155–162. <https://doi.org/https://doi.org/10.1016/j.proeng.2012.01.1188>
- Burns, R.T., Moody, L.B., Celen, I., Buchanan, J.R., 2003. Optimization of phosphorus precipitation from swine manure slurries to enhance recovery. *Water Sci. Technol.*
- Burton, C.H., Turner, C., Arkhipchenko, I.A., Beck, J., Bernal, M., Bicudo, J., Böhm, R., Bogun, G., Carton, O., Dohanyos, M., Geers, R., Georgacakis, D., Hahne, J., Hayes, M., Heinonen-



Tanski, H., Martens, W., Melse, R.W., Menzi, H., B. Møller, H., Williams, S., 2003. Manure management : treatment strategies for sustainable agriculture - 2nd ed / [edited by] C.H.

Burton and C. Turner Author(s) Burton, C.H. ; Turner, C. Publisher Silsoe : Silsoe Research Institute Publication year 2003 Description xxvii, 451 p Notes Pre.

Cayuela, M.L., Oenema, O., Kuikman, P.J., Bakker, R.R., Van Groenigen, J.W., 2010. Bioenergy by-products as soil amendments? Implications for carbon sequestration and greenhouse gas emissions. *GCB Bioenergy* 2, 201–213. <https://doi.org/10.1111/j.1757-1707.2010.01055.x>

Cerrillo, M., Palatsi, J., Comas, J., Vicens, J., Bonmatí, A., 2015. Struvite precipitation as a technology to be integrated in a manure anaerobic digestion treatment plant – removal efficiency, crystal characterization and agricultural assessment. *J. Chem. Technol. Biotechnol.* 90, 1135–1143. <https://doi.org/10.1002/jctb.4459>

Chavan, R.B., Arega, Y., 2018. Advance Research in Textile Engineering Electrocoagulation Followed by Ion Exchange or Membrane Separation Techniques for Recycle of Textile Wastewater. *Adv Res Text Eng.* 3, 1024.

Cieślik, B., Konieczka, P., 2017. A review of phosphorus recovery methods at various steps of wastewater treatment and sewage sludge management. The concept of “no solid waste generation” and analytical methods. *J. Clean. Prod.* 142, 1728–1740. <https://doi.org/10.1016/j.jclepro.2016.11.116>

Cordell, D., Rosemarin, A., Schröder, J.J., Smit, A.L., 2011. Towards global phosphorus security: A systems framework for phosphorus recovery and reuse options. *Chemosphere* 84, 747–758. <https://doi.org/https://doi.org/10.1016/j.chemosphere.2011.02.032>

Council of the European Communities, 1991. Directive concerning the collection, treatment and discharge of urban wastewater and the discharge of wastewater from certain industrial sectors (91/271/EEC). *Off J Eur Communities Ser L* 135–140.

Crutchik, D., Rodrigues, S., Ruddle, D., Garrido, J.M., 2018. Evaluation of a low-cost magnesium

- product for phosphorus recovery by struvite crystallization. *J. Chem. Technol. Biotechnol.* 93, 1012–1021. <https://doi.org/10.1002/jctb.5453>
- De-Bashan, L.E., Bashan, Y., 2004. Recent advances in removing phosphorus from wastewater and its future use as fertilizer (1997-2003). *Water Res.* 38, 4222–4246. <https://doi.org/10.1016/j.watres.2004.07.014>
- Desmidt, E., Ghyselbrecht, K., Zhang, Y., Pinoy, L., Van Der Bruggen, B., Verstraete, W., Rabaey, K., Meesschaert, B., 2015. Global phosphorus scarcity and full-scale P-recovery techniques: A review. *Crit. Rev. Environ. Sci. Technol.* 45, 336–384. <https://doi.org/10.1080/10643389.2013.866531>
- Doyle, J.D., Oldring, K., Churchley, J., Price, C., 2003. Chemical Control of Struvite Precipitation. *J. Environ. Eng.* 129.
- Durrant, A.E., Scrimshaw, M.D., Stratful, I., Lester, J.N., 1999. Review of the Feasibility of Recovering Phosphate from Wastewater for Use as a Raw Material by the Phosphate Industry. *Environ. Technol.* 20, 749–758. <https://doi.org/10.1080/09593332008616870>
- Dyhrman, S.T., Mooy, V., Devol, A., 2007. Microbes and the Marine Phosphorus Cycle. *Oceanography* 20, 110–116.
- Egle, L., Rechberger, H., Krampe, J., Zessner, M., 2016. Phosphorus recovery from municipal wastewater: An integrated comparative technological, environmental and economic assessment of P recovery technologies. *Sci. Total Environ.* 571, 522–542. <https://doi.org/10.1016/j.scitotenv.2016.07.019>
- Etter, B., Tilley, E., Khadka, R., Udert, K.M., 2011. Low-cost struvite production using source-separated urine in Nepal. *Water Res.* 45, 852–862. <https://doi.org/10.1016/j.watres.2010.10.007>
- Eurostat - Statistic explained, n.d. No Title [WWW Document]. URL [https://ec.europa.eu/eurostat/statistics-explained/index.php/Main\\_Page](https://ec.europa.eu/eurostat/statistics-explained/index.php/Main_Page)

- Evanylo, G., Sherony, C., Spargo, J., Starner, D., Brosius, M., Haering, K., 2008. Soil and water environmental effects of fertilizer-, manure-, and compost-based fertility practices in an organic vegetable cropping system. *Agric. Ecosyst. Environ.* 127, 50–58.  
<https://doi.org/https://doi.org/10.1016/j.agee.2008.02.014>
- Fang, C., Zhang, T., Jiang, R., Ohtake, H., 2016. Phosphate enhance recovery from wastewater by mechanism analysis and optimization of struvite settleability in fluidized bed reactor. *Sci. Rep.* 6, 32215.
- FAO, 2017. World fertilizer trends and outlook to 2018. Food Agric. Organ. United Nations 66.
- Fernandes, G.W., Kunz, A., Steinmetz, R.L.R., Szogi, A., Vanotti, M., de Moraes Flores, É.M., Dressler, V.L., 2012. Chemical phosphorus removal: a clean strategy for piggery wastewater management in Brazil. *Environ. Technol.* 33, 1677–1683.  
<https://doi.org/10.1080/09593330.2011.642896>
- Fleming, R., Ford, M., 2001. Human versus Animals - Comparison of Waste Properties. *Beef* 8–11.
- Foerid, B., 2015. Biochar in Nutrient Recycling—The Effect and Its Use in Wastewater Treatment. *Open J. Soil Sci.* 05, 39–44. <https://doi.org/10.4236/ojss.2015.52004>
- Fukumoto, Y., Suzuki, K., Kuroda, K., Waki, M., Yasuda, T., 2011. Effects of struvite formation and nitrification promotion on nitrogenous emissions such as NH<sub>3</sub>, N<sub>2</sub>O and NO during swine manure composting. *Bioresour. Technol.* 102, 1468–1474.  
<https://doi.org/https://doi.org/10.1016/j.biortech.2010.09.089>
- Gaterell, M.R., Gay, R., Wilson, R., Gochin, R.J., Lester, J.N., 2000. An Economic and Environmental Evaluation of the Opportunities for Substituting Phosphorus Recovered from Wastewater Treatment Works in Existing UK Fertiliser Markets. *Environ. Technol.* 21, 1067–1084. <https://doi.org/10.1080/09593332108618050>
- Guedes, P., Couto, N., Ottosen, L.M., Ribeiro, A.B., 2014. Phosphorus recovery from sewage sludge ash through an electrodialytic process. *Waste Manag.* 34, 886–892.

<https://doi.org/https://doi.org/10.1016/j.wasman.2014.02.021>

Hakizimana, J.N., Gourich, B., Chafi, M., Stiriba, Y., Vial, C., Drogui, P., Naja, J., 2017.

Electrocoagulation process in water treatment: A review of electrocoagulation modeling approaches. *Desalination* 404, 1–21. <https://doi.org/10.1016/j.desal.2016.10.011>

Hall, H., Abell, A., 2006. New role realities: Avenues for extending the reach of information specialists. *Proc. Am. Soc. Inf. Sci. Technol.* 43, 1–13.

Havukainen, J., Nguyen, M.T., Hermann, L., Horttanainen, M., Mikkilä, M., Deviatkin, I.,

Linnanen, L., 2016. Potential of phosphorus recovery from sewage sludge and manure ash by thermochemical treatment. *Waste Manag.* 49, 221–229.

<https://doi.org/10.1016/j.wasman.2016.01.020>

He, S., Zhang, Y., Yang, M., Du, W., Harada, H., 2007. Repeated use of MAP decomposition

residues for the removal of high ammonium concentration from landfill leachate. *Chemosphere* 66, 2233–2238. <https://doi.org/https://doi.org/10.1016/j.chemosphere.2006.09.016>

Hernandez, J.A., Schmitt, M.A., 2012. Manure management in Minnesota, Publ. WW- 03553. Rev.,

Hu, B., 2016. Recovery of phosphorus and fine particles as fertilizer from swine manure by electrocoagulation 1–24.

Huang, H., Song, Q., Wang, W., Wu, S., Dai, J., 2012. Treatment of anaerobic digester effluents of nylon wastewater through chemical precipitation and a sequencing batch reactor process. *J. Environ. Manage.* 101, 68–74. <https://doi.org/https://doi.org/10.1016/j.jenvman.2011.12.035>

<https://doi.org/https://doi.org/10.1016/j.jenvman.2011.12.035>

Huang, H., Xu, C., Zhang, W., 2011. Removal of nutrients from piggery wastewater using struvite precipitation and pyrogenation technology. *Bioresour. Technol.* 102, 2523–2528.

<https://doi.org/https://doi.org/10.1016/j.biortech.2010.11.054>

Huang, H.M., Xiao, X.M., Yang, L.P., Yan, B., 2011. Removal of ammonium from rare-earth wastewater using natural brucite as a magnesium source of struvite precipitation. *Water Sci. Technol.* 63, 468–474. <https://doi.org/10.2166/wst.2011.245>

<https://doi.org/10.2166/wst.2011.245>

- Hutnan, M., Drtil, M., Kalina, A., 2006. Anaerobic stabilisation of sludge produced during municipal wastewater treatment by electrocoagulation. *J. Hazard. Mater.* 131, 163–169. <https://doi.org/10.1016/j.jhazmat.2005.09.032>
- IFA, 2014. Fertilizer Outlook 2014-2018. 82nd IFA Annu. Conf. Sydney 1–7.
- Inan, H., Alaydin, E., 2014. Phosphate and nitrogen removal by iron produced in electrocoagulation reactor. *Desalin. Water Treat.* 52, 1396–1403. <https://doi.org/10.1080/19443994.2013.787950>
- Jadhav, D.A., Ghosh Ray, S., Ghangrekar, M.M., 2017. Third generation in bio-electrochemical system research – A systematic review on mechanisms for recovery of valuable by-products from wastewater. *Renew. Sustain. Energy Rev.* 76, 1022–1031. <https://doi.org/10.1016/j.rser.2017.03.096>
- Jaffer, Y., Clark, T.A., Pearce, P., Parsons, S.A., 2002. Potential phosphorus recovery by struvite formation. *Water Res.* 36, 1834–1842. [https://doi.org/10.1016/S0043-1354\(01\)00391-8](https://doi.org/10.1016/S0043-1354(01)00391-8)
- Johnston, A.E., Richards, I.R., 2003. Effectiveness of different precipitated phosphates as phosphorus sources for plants. *Soil Use Manag.* 19, 45–49. <https://doi.org/10.1111/j.1475-2743.2003.tb00278.x>
- Jordaan, E.M., Ackerman, J., Cicek, N., 2009. Nutrient Management in Wastewater Treatment Processes 1033–1042.
- Kataki, S., West, H., Clarke, M., Baruah, D.C., 2016a. Phosphorus recovery as struvite from farm, municipal and industrial waste: Feedstock suitability, methods and pre-treatments. *Waste Manag.* 49, 437–454. <https://doi.org/10.1016/j.wasman.2016.01.003>
- Kataki, S., West, H., Clarke, M., Baruah, D.C., 2016b. Phosphorus recovery as struvite: Recent concerns for use of seed, alternative Mg source, nitrogen conservation and fertilizer potential. *Resour. Conserv. Recycl.* 107, 142–156. <https://doi.org/10.1016/j.resconrec.2015.12.009>
- Kiran, Y.K., Barkat, A., CUI, X. qiang, FENG, Y., PAN, F. shan, TANG, L., YANG, X. e., 2017. Cow manure and cow manure-derived biochar application as a soil amendment for reducing

- cadmium availability and accumulation by *Brassica chinensis* L. in acidic red soil. *J. Integr. Agric.* 16, 725–734. [https://doi.org/10.1016/S2095-3119\(16\)61488-0](https://doi.org/10.1016/S2095-3119(16)61488-0)
- Kumashiro, K., Ishiwatari, H., Nawamura, Y., 2001. A pilot plant study on using seawater as a magnesium source for struvite precipitation, in: *Second International Conference about P-Recovery*—submitted.
- Le Corre, K.S., Valsami-Jones, E., Hobbs, P., Parson, S.A., 2005. Nutrient Management in Wastewater Treatment Processes and Recycle Streams 1415–1419.
- Le Corre, K.S., Valsami-Jones, E., Hobbs, P., Parsons, S.A., 2009. Phosphorus Recovery from Wastewater by Struvite Crystallization: A Review. *Crit. Rev. Environ. Sci. Technol.* 39, 433–477. <https://doi.org/10.1080/10643380701640573>
- Lee, S.I., Weon, S.Y., Lee, C.W., Koopman, B., 2003. Removal of nitrogen and phosphate from wastewater by addition of bittern. *Chemosphere* 51, 265–271. [https://doi.org/10.1016/S0045-6535\(02\)00807-X](https://doi.org/10.1016/S0045-6535(02)00807-X)
- Lehmann, J., 2009. Biological carbon sequestration must and can be a win-win approach. *Clim. Change* 97, 459–463. <https://doi.org/10.1007/s10584-009-9695-y>
- Li, B., Boiarkina, I., Yu, W., Huang, H.M., Munir, T., Wang, G.Q., Young, B.R., 2019. Phosphorous recovery through struvite crystallization: Challenges for future design. *Sci. Total Environ.* 648, 1244–1256. <https://doi.org/https://doi.org/10.1016/j.scitotenv.2018.07.166>
- Li, X.Z., Zhao, Q.L., 2003. Recovery of ammonium-nitrogen from landfill leachate as a multi-nutrient fertilizer. *Ecol. Eng.* 20, 171–181. [https://doi.org/https://doi.org/10.1016/S0925-8574\(03\)00012-0](https://doi.org/https://doi.org/10.1016/S0925-8574(03)00012-0)
- Liu, Z., Singer, S., Tong, Y., Kimbell, L., Anderson, E., Hughes, M., Zitomer, D., McNamara, P., 2018. Characteristics and applications of biochars derived from wastewater solids. *Renew. Sustain. Energy Rev.* 90, 650–664. <https://doi.org/https://doi.org/10.1016/j.rser.2018.02.040>
- Lorenzen, C.J., 1965. Determination fo Chlorophyll and Pheophytin Pigments. *Plant Physiol.* 343–

346.

- Lǔ, J., Liu, H., Liu, R., Zhao, X., Sun, L., Qu, J., 2013. Adsorptive removal of phosphate by a nanostructured Fe-Al-Mn trimetal oxide adsorbent. *Powder Technol.* 233, 146–154. <https://doi.org/10.1016/j.powtec.2012.08.024>
- Makara, A., Kowalski, Z., 2015. Pig manure treatment and purification by filtration. *J. Environ. Manage.* 161, 317–324. [https://doi.org/https://doi.org/10.1016/j.jenvman.2015.07.022](https://doi.org/10.1016/j.jenvman.2015.07.022)
- Marchi, A., Geerts, S., Weemaes, M., Wim, S., Christine, V., 2015. Full-scale phosphorus recovery from digested waste water sludge in Belgium - Part I: Technical achievements and challenges. *Water Sci. Technol.* 71, 487–494. <https://doi.org/10.2166/wst.2015.023>
- Masebinu, S.O., Akinlabi, E.T., Muzenda, E., Aboyade, A.O., 2019. A review of biochar properties and their roles in mitigating challenges with anaerobic digestion. *Renew. Sustain. Energy Rev.* 103, 291–307. [https://doi.org/https://doi.org/10.1016/j.rser.2018.12.048](https://doi.org/10.1016/j.rser.2018.12.048)
- Matsumiya, Y., Yamasita, T., Nawamura, Y., 2000. Phosphorus Removal from Sidestreams by Crystallisation of Magnesium-Ammonium-Phosphate Using Seawater. *Water Environ. J.* 14, 291–296. <https://doi.org/10.1111/j.1747-6593.2000.tb00263.x>
- Mekonnen, M.M., Hoekstra, A.Y., 2018. Global Anthropogenic Phosphorus Loads to Freshwater and Associated Grey Water Footprints and Water Pollution Levels: A High-Resolution Global Study. *Water Resour. Res.* 54, 345–358. <https://doi.org/10.1002/2017WR020448>
- Merino-Jimenez, I., Celorrio, V., Fermin, D.J., Greenman, J., Ieropoulos, I., 2017. Enhanced MFC power production and struvite recovery by the addition of sea salts to urine. *Water Res.* 109, 46–53. <https://doi.org/10.1016/j.watres.2016.11.017>
- Møller, H.B., Hansen, J.D., Sørensen, C.A.G., 2007. Nutrient recovery by solid-liquid separation and methane productivity of solids. *Trans. ASABE* 50, 193–200.
- Mores, R., Treichel, H., Zakrzewski, C.A., Kunz, A., Steffens, J., Dallago, R.M., 2016. Remove of phosphorous and turbidity of swine wastewater using electrocoagulation under continuous

flow. *Sep. Purif. Technol.* 171, 112–117.

<https://doi.org/https://doi.org/10.1016/j.seppur.2016.07.016>

Münch, E. V, Barr, K., 2001. Controlled struvite crystallisation for removing phosphorus from anaerobic digester sidestreams. *Water Res.* 35, 151–159.

[https://doi.org/https://doi.org/10.1016/S0043-1354\(00\)00236-0](https://doi.org/https://doi.org/10.1016/S0043-1354(00)00236-0)

Nakakubo, T., Tokai, A., Ohno, K., 2012. Comparative assessment of technological systems for recycling sludge and food waste aimed at greenhouse gas emissions reduction and phosphorus recovery. *J. Clean. Prod.* 32, 157–172.

<https://doi.org/https://doi.org/10.1016/j.jclepro.2012.03.026>

Nghiem, L.D., Koch, K., Bolzonella, D., Drewes, J.E., 2017. Full scale co-digestion of wastewater sludge and food waste: Bottlenecks and possibilities. *Renew. Sustain. Energy Rev.* 72, 354–

362. <https://doi.org/https://doi.org/10.1016/j.rser.2017.01.062>

Nguyen, D.-D., Kim, S.-D., Yoon, Y.-S., 2014. Enhanced phosphorus and COD removals for retrofit of existing sewage treatment by electrocoagulation process with cylindrical aluminum electrodes. *Desalin. Water Treat.* 52, 2388–2399.

<https://doi.org/10.1080/19443994.2013.794707>

Olsen, S.R., Cole, C. V., Watanabe, F.S., Dean, L.A., 1954. Estimation of available phosphorus in soils by extraction with NaHCO<sub>3</sub>. *USDA Cir.*939.

Omwene, P.I., Koby, M., Can, O.T., 2018. Phosphorus removal from domestic wastewater in electrocoagulation reactor using aluminium and iron plate hybrid anodes. *Ecol. Eng.* 123, 65–

73. <https://doi.org/10.1016/j.ecoleng.2018.08.025>

Ozyonar, F., Karagozoglu, B., 2011. Operating cost analysis and treatment of domestic wastewater by electrocoagulation using aluminum electrodes. *Polish J. Environ. Stud.* 20, 173–179.

Parliament, E.U., 2012. REGULATION (EU) No 259/2012. *Off. J. Eur. Union* 94, 16–21.

Pastor, L., Marti, N., Bouzas, A., Seco, A., 2008. Sewage sludge management for phosphorus



- recovery as struvite in EBPR wastewater treatment plants. *Bioresour. Technol.* 99, 4817–4824.  
<https://doi.org/https://doi.org/10.1016/j.biortech.2007.09.054>
- Pepè Sciarria, T., Vacca, G., Tambone, F., Trombino, L., Adani, F., 2018. Nutrient recovery and energy production from digestate using microbial electrochemical technologies (METs). *J. Clean. Prod.* 208, 1022–1029. <https://doi.org/10.1016/J.JCLEPRO.2018.10.152>
- Prywer, J., Torzewska, A., Płociński, T., 2012. Unique surface and internal structure of struvite crystals formed by *Proteus mirabilis*. *Urol. Res.* 40, 699–707. <https://doi.org/10.1007/s00240-012-0501-3>
- Quist-Jensen, C.A., Jørgensen, M.K., Christensen, M.L., 2016. Treated seawater as a magnesium source for phosphorous recovery from wastewater—A feasibility and cost analysis. *Membranes (Basel)*. 6. <https://doi.org/10.3390/membranes6040054>
- Rahaman, M.S., Mavinic, D.S., Meikleham, A., Ellis, N., 2014. Modeling phosphorus removal and recovery from anaerobic digester supernatant through struvite crystallization in a fluidized bed reactor. *Water Res.* 51, 1–10. <https://doi.org/https://doi.org/10.1016/j.watres.2013.11.048>
- Rittmann, B.E., Mayer, B., Westerhoff, P., Edwards, M., 2011. Capturing the lost phosphorus. *Chemosphere* 84, 846–853. <https://doi.org/10.1016/j.chemosphere.2011.02.001>
- Rouff, A.A., 2013. Temperature-dependent phosphorus precipitation and chromium removal from struvite-saturated solutions. *J. Colloid Interface Sci.* 392, 343–348.  
<https://doi.org/https://doi.org/10.1016/j.jcis.2012.10.013>
- Schoumans, O.F., Ehlert, P.A.I., Regelink, I.C., Nelemans, J.A., Noij, I.G.A.M., Van Tintelen, W., Rulkens, W.H., 2017. Chemical phosphorus recovery from animal manure and digestate.
- Schoumans, O.F., Nelemans, J.A., Tintelen, W. Van, Rulkens, W.H., Oenema, O., 2014. Explorative study of phosphorus recovery from pig slurry 50.
- Schoumans, O.F., Rulkens, W.H., Oenema, O., Ehlert, P. a I., 2010. Phosphorus recovery from animal manure. *Alterra Rep.* 2158. <https://doi.org/ISSN:1566-7197>

- Seitzinger, S.P., Mayorga, E., Bouwman, A.F., Kroeze, C., Beusen, A.H.W., Billen, G., Van Drecht, G., Dumont, E., Fekete, B.M., Garnier, J., Harrison, J.A., 2010. Global river nutrient export: A scenario analysis of past and future trends. *Global Biogeochem. Cycles* 24. <https://doi.org/10.1029/2009GB003587>
- Shih, K., Yan, H., 2016. Chapter 26 - The Crystallization of Struvite and Its Analog (K-Struvite) From Waste Streams for Nutrient Recycling, in: Prasad, M.N. V, Shih, K.B.T.-E.M. and W. (Eds.), . Academic Press, pp. 665–686. <https://doi.org/10.1016/B978-0-12-803837-6.00026-3>
- Shin, H.S., Lee, S.M., 1998. Removal of Nutrients in Wastewater by using Magnesium Salts. *Environ. Technol.* 19, 283–290. <https://doi.org/10.1080/09593331908616682>
- Smit, A.L., van Middelkoop, J.C., van Dijk, W., van Reuler, H., 2015. A substance flow analysis of phosphorus in the food production, processing and consumption system of the Netherlands. *Nutr. Cycl. Agroecosystems* 103, 1–13. <https://doi.org/10.1007/s10705-015-9709-2>
- Soare, A., Lakerveld, R., van Royen, J., Zocchi, G., Stankiewicz, A.I., Kramer, H.J.M., 2012. Minimization of Attrition and Breakage in an Airlift Crystallizer. *Ind. Eng. Chem. Res.* 51, 10895–10909. <https://doi.org/10.1021/ie300432w>
- Sørensen, B.L., Dall, O.L., Habib, K., 2015. Environmental and resource implications of phosphorus recovery from waste activated sludge. *Waste Manag.* 45, 391–399. <https://doi.org/10.1016/j.wasman.2015.02.012>
- Spokas, K.A., Reicosky, D.C., 2009. Impacts of sixteen different biochars on soil greenhouse gas production 3, 179–193.
- Stafford, B., Dotro, G., Vale, P., Jefferson, B., Jarvis, P., 2014. Removal of phosphorus from trickling filter effluent by electrocoagulation. *Environ. Technol.* 35, 3139–3146. <https://doi.org/10.1080/09593330.2014.932440>
- Steinbeiss, S., Gleixner, G., Antonietti, M., 2009. Effect of biochar amendment on soil carbon

balance and soil microbial activity. *Soil Biol. Biochem.* 41, 1301–1310.

<https://doi.org/https://doi.org/10.1016/j.soilbio.2009.03.016>

Stolzenburg, P., Capdevielle, A., Teychené, S., Biscans, B., 2014. Struvite precipitation with MgO as a precursor: Application to wastewater treatment. *Chem. Eng. Sci.* 133, 9–15.

<https://doi.org/10.1016/j.ces.2015.03.008>

Stratful, I., Scrimshaw, M.D., Lester, J.N., 2004. Removal of Struvite to Prevent Problems Associated with Its Accumulation in Wastewater Treatment Works. *Water Environ. Res.* 76, 437–443.

Strickland, J.D.H., Parsons, T.R., 1968. A Practical Handbook of Seawater Analysis. *Bull. Fish. Res. Board Canada* 167, 1–311.

Stumpf, D., Zhu, H., Heinzmann, B., Kraume, M., 2008. Phosphorus recovery in aerated systems by MAP precipitation: optimizing operational conditions. *Water Sci. Technol.* 58, 1977–1983.

<https://doi.org/10.2166/wst.2008.549>

Suci Perwitasari, D., Edahwati, L., Sutiyono, S., Karaman, N., Jamari, J., Muryanto, S., Bayuseno, A., 2016. Effect of Calcium Additive on the Crystallization of Struvite. *MATEC Web Conf.*

58, 1007. <https://doi.org/10.1051/matecconf/20165801007>

Symonds, E.M., Cook, M.M., McQuaig, S.M., Ulrich, R.M., Schenck, R.O., Lukasik, J.O., Van Vleet, E.S., Breitbart, M., 2015. Reduction of nutrients, microbes, and personal care products in domestic wastewater by a benchtop electrocoagulation unit. *Sci. Rep.* 5, 1–8.

<https://doi.org/10.1038/srep09380>

Szögi, A.A., Vanotti, M.B., Hunt, P.G., 2015. Phosphorus recovery from pig manure solids prior to land application. *J. Environ. Manage.* 157, 1–7. <https://doi.org/10.1016/j.jenvman.2015.04.010>

Szogi, A.A., Vanotti, M.B., Ro, K.S., 2015. Methods for Treatment of Animal Manures to Reduce Nutrient Pollution Prior to Soil Application. *Curr. Pollut. Reports* 1, 47–56.

<https://doi.org/10.1007/s40726-015-0005-1>

- Tambone, F., Orzi, V., D'Imporzano, G., Adani, F., 2017. Solid and liquid fractionation of digestate: Mass balance, chemical characterization, and agronomic and environmental value. *Bioresour. Technol.* 243, 1251–1256. <https://doi.org/10.1016/j.biortech.2017.07.130>
- Tarragó, E., Puig, S., Rusalleda, M., Balaguer, M.D., Colprim, J., 2016. Controlling struvite particles' size using the up-flow velocity. *Chem. Eng. J.* 302, 819–827. <https://doi.org/10.1016/j.cej.2016.06.036>
- Tarragó, E., Sciarria, T.P., Rusalleda, M., Colprim, J., Balaguer, M.D., Adani, F., Puig, S., 2018. Effect of suspended solids and its role on struvite formation from digested manure. *J. Chem. Technol. Biotechnol.* <https://doi.org/10.1002/jctb.5651>
- Tchamango, S., Nanseu-Njiki, C.P., Ngameni, E., Hadjiev, D., Darchen, A., 2010. Treatment of dairy effluents by electrocoagulation using aluminium electrodes. *Sci. Total Environ.* 408, 947–952. <https://doi.org/10.1016/j.scitotenv.2009.10.026>
- U.S. Geological Survey, n.d. USGS Mineral Commodities Summary, [http://minerals.usgs.gov/minerals/pubs/commodity/phosphate\\_rock/](http://minerals.usgs.gov/minerals/pubs/commodity/phosphate_rock/) [WWW Document].
- Ueno, Y., Fujii, M., 2001. Three Years Experience of Operating and Selling Recovered Struvite from Full-Scale Plant. *Environ. Technol.* 22, 1373–1381. <https://doi.org/10.1080/09593332208618196>
- United Nations, Department of Economic and Social Affairs, P.D., 2019. No Title [WWW Document]. URL <http://www.un.org/en/development/desa/population/>
- Uysal, A., Yilmazel, Y.D., Demirer, G.N., 2010. The determination of fertilizer quality of the formed struvite from effluent of a sewage sludge anaerobic digester. *J. Hazard. Mater.* 181, 248–254. <https://doi.org/10.1016/j.jhazmat.2010.05.004>
- Vaccari, D., Daneshgar, S., Callegari, A., Capodaglio, A.G., 2018. The Potential Phosphorus Crisis : Resource Conservation and Possible Escape Technologies : A Review. *Resources* 7, 37. <https://doi.org/10.3390/resources7020037>

- Vanotti, M., Szogi, A., 2009. Technology for recovery of phosphorus from animal wastewater through calcium phosphate precipitation. *Proc. Int. Conf. Nutr. Recover. from Wastewater Syst.* 459–468.
- Vanotti, M.B., Szogi, A.A., Hunt, P.G., 2003. Extraction of soluble phosphorus from swine wastewater. *Am. Soc. Agric. Eng.* 46, 1665–1674.
- Wang, X., Selvam, A., Chan, M., Wong, J.W.C., 2013. Nitrogen conservation and acidity control during food wastes composting through struvite formation. *Bioresour. Technol.* 147, 17–22.  
<https://doi.org/https://doi.org/10.1016/j.biortech.2013.07.060>
- Williams, S., 1999. Struvite Precipitation in the Sludge Stream at Slough Wastewater Treatment Plant and Opportunities for Phosphorus Recovery. *Environ. Technol.* 20, 743–747.  
<https://doi.org/10.1080/09593332008616869>
- Wilsenach, J.A., Schuurbiens, C.A.H., van Loosdrecht, M.C.M., 2007. Phosphate and potassium recovery from source separated urine through struvite precipitation. *Water Res.* 41, 458–466.  
<https://doi.org/https://doi.org/10.1016/j.watres.2006.10.014>
- Yan, H., Shih, K., 2016. Effects of calcium and ferric ions on struvite precipitation: A new assessment based on quantitative X-ray diffraction analysis. *Water Res.* 95, 310–318.  
<https://doi.org/https://doi.org/10.1016/j.watres.2016.03.032>
- Yetilmezsoy, K., Ilhan, F., Kocak, E., Akbin, H.M., 2017. Feasibility of struvite recovery process for fertilizer industry: A study of financial and economic analysis. *J. Clean. Prod.* 152, 88–102.  
<https://doi.org/10.1016/j.jclepro.2017.03.106>
- Zhang, H., Johnson, G., Fram, M., 2003. *Managing Phosphorus from Animal Manure.*
- Zhang, X., Lin, H., Hu, B., 2018. The effects of electrocoagulation on phosphorus removal and particle settling capability in swine manure. *Sep. Purif. Technol.* 200, 112–119.  
<https://doi.org/10.1016/j.seppur.2018.02.025>
- Zhang, X., Lin, H., Hu, B., 2016. Phosphorus removal and recovery from dairy manure by

electrocoagulation. RSC Adv. 6, 57960–57968. <https://doi.org/10.1039/C6RA06568F>